April 2016

Design and Optimization of a Baja SAE Vehicle 2015-2016

Dylan Craig Stimson
Worcester Polytechnic Institute

Jason Nitin Mehta
Worcester Polytechnic Institute

Kenneth William McPherson
Worcester Polytechnic Institute

Ryan Sedghi Horton
Worcester Polytechnic Institute

2015-2016 SAE Baja Major Qualifying Project Final Report

Written by:
Dylan Stimson, Jason Mehta, Kenneth McPherson, Ryan Horton

Submitted to:
Professor David Planchard

Submitted on:
04/28/2016

Table of Contents

Abstract 5
Acknowledgements 6
Introduction 7
Background 8
Components of a Baja Vehicle 8
Steering System 8
Suspension 11
Control Arms 13
Brakes 16
Engine and Drivetrain 17
Methodology and Procedures 17
Suspension and Steering 17
Camber 17
Front Control Arms 19
Tie Rods and Linkages 28
Caster & Steering Axis Inclination 28
Ackerman Steering 28
Steering Restrictions 30
Steering Column Assembly and Mounting 31
Rear Control Arms 33
Mechatronic Analysis of Suspension 36
Frame 39
Seating 40
Body Panels 41
Brakes 42
Drive Train 42
Drivetrain Modifications 45
Drivetrain Mounting 49
Drivetrain Orientation 53
Throttle Assembly 54

Circuitry 56
Recommendations and Conclusions 58
Suspension 58
Shifting Linkage 59
Additional Safety Features 59
Body Panels 59
Rear Tow Hitch 59
Steering Wheel Adapter 59
Brakes 59
Appendix A: Relevant 2016 SAE Baja Competition Rules 60
Article 3: Electrical System 60
Section B3.1 General Electrical System Overview NEW 60
Section B3.3.1 Kill Switch – Type NEW 60
Section B3.6 Reverse Light and Alarm NEW 60
Article 4: Towing Hitch Point 60
Section B4.2.2 60
Article 11: Braking System 61
Section B11.1 Foot Brake 61
Section B11.2 Independent Brake Circuits 61
Appendix B: Shock and Spring Prices 62
Table 1: Polaris Shocks and Springs 62
Table 2: Fox Shocks and Springs 62
Table 3: Comparative Analysis of Fox, Polaris, and Rad-Flo Shocks and Springs 62
Appendix C: Vehicle Speed and Torque with Final Drive Table 63
Appendix D: Hill Climb Results 65
Appendix E: State Equations from Mechatronic Analysis of Front and Rear Suspensions 66
Appendix F: Works Cited 68

Table of Figures

Figure 1: Visual Representation of Camber 8

Figure 2: Visual Representation of Caster 9
Figure 3: Visual Representation of SAI 10
Figure 4: Ackerman Steering Principle 10
Figure 5: Diagram of Steering Angle 11
Figure 6: Coil-Over Shock (Left) versus an Air-Shock (Right) 12
Figure 7: Macpherson Strut 14
Figure 8: Double Wishbone Suspension 15
Figure 9: Trailing and Semi-Trailing Arm Suspension 15
Figure 10: Floating Caliper Disk Brake 16
Figure 11: PMKS Model of Control Arms 18
Figure 12: Front Wheel Hub Assembly 19
Figure 13: Control Arm Solution 1 20
Figure 14: Custom Knuckle Design 21
Figure 15: CAD Model of KFX-400 Spindle 22
Figure 16: 2004 KFX-400 Spindle 23
Figure 17: 2004 KFX-400 Spindle 23
Figure 18: 2004 KFX-2004 Hub 24
Figure 19: 2004 KFX-400 Hub Assembly 24
Figure 20: 2004 KFX-400 Hub Assembly Mounted to Rim 25
Figure 21: 2004 KFX-400 Hub Assembly Mounted to Rim 25
Figure 22: Graphical Analysis 27
Figure 23: Completed Front Suspension 28
Figure 24: Side View of Wheel Spacer and Hub Assembly 30
Figure 25: Complete Tire, Wheel Spacer, and Hub Assembly 31
Figure 26: Double U Joint Steering Column Configuration 32
Figure 27: Complete Mounted Steering Column 33
Figure 28: Close Up of Oval Flange Bearing Mounted to Chassis Tab 33
Figure 29: Redesigned Rear Frame 34
Figure 30: Actual Frame after Hubb Equipment Welding 34
Figure 31: Redesigned Rear, Upper Control Arms 35
Figure 32: Redesigned Rear Control Arms 35
Figure 33: Finalized Rear Suspension 36
Figure 34: Finalized Rear Suspension 36
Figure 35: Free Body Diagrams of Half Car Model 37
Figure 36: Causal Bond Graph 37
Figure 37: Causal Bond Graph with State Variables 38
Figure 38: Drawing of Front Hitch 39
Figure 39: Front Hitch Point Welded by Hubb Equipment 40
Figure 40: Maximum Displacement of Seat Mount 41
Figure 41: Von Mises Stress in Seat Mount 41

Figure 42: Completed Panels on Vehicle 42
Figure 43: CVT Mounted to the Model 20 Engine 43
Figure 44: Visualization of Hill Climb 45
Figure 45: Drawing of Original Drive CVT Flange 46
Figure 46: Drawing of Modified CVT Flange 46
Figure 47: Bored CVT 47
Figure 48: CVT Attached to FNR 47
Figure 49: FNR Female Spline 48
Figure 50: Detailed View of Half Shaft with Adapter 48
Figure 51: Fitment of Half Shafts with FNR 49
Figure 52: Engine Mount Drawing 49
Figure 53: Maximum Displacement of Engine Mount 50
Figure 54: Von Mises Stress of Engine Mount 50
Figure 55: FNR Mount CAD Model 51
Figure 56: Maximum Displacement of FNR Mount 51
Figure 57: Von Mises Stress of FNR Mount 51
Figure 58: Front FNR Mounting Tab 52
Figure 59: Rear FNR Mounting Tabs 52
Figure 60: Engine and FNR Mount Mounting Tabs 53
Figure 61: Drivetrain Orientation 53
Figure 62: Final Orientation of Drivetrain 54
Figure 63: Unmodified Foot Control Linkage 55
Figure 64: Modified Foot Control Linkage 55
Figure 65: Modified Foot Control 55
Figure 66: Throttle Cable Mounting System 56
Figure 67: BSAE Circuit Diagram 57
Figure 68: Kill Switch Circuit Diagram 58
Figure 69: Rear Tow Hitch Point Drawing 61

Abstract

The purpose of the Society of Automotive Engineers (SAE) Baja MQP was to update and modify the pre-existing vehicle for competition in 2017. Major design modifications were made to the chassis, suspension, drivetrain, and steering.

The rear of the chassis was modified allowing for proper orientation of the drivetrain and suspension. Kinematic analysis was performed during the design phase for the front and rear suspension in order to ensure ideal camber throughout suspension travel. The entire suspension was then represented utilizing the half car model, analyzed using the mechatronic bond-graph method, and simulated using Matlab.

The team used stress analysis to ensure that all designed components could withstand the rigors of an SAE Baja competition without component failure. Physical analysis was conducted to find the appropriate gear reduction required to meet our design specifications for top speed and maximum torque.

The team worked diligently with manufacturers to ensure that the components could be manufactured and used the WPI SAE chapter to ensure that the car was completed in a timely fashion. Engineering analysis as well as diligent communication with all stakeholders allowed the MQP to create a fully operational and competitive vehicle that meets the Mini Baja SAE competition specifications.

Acknowledgements

The 2015-2016 SAE Baja team would like to thank the following people for their contributions to this MQP:

- Professor Planchard for his effort in pushing us to our limits and advising us to produce the best vehicle possible. He was vital in our engineering design and in bringing both the Formula and Baja teams together within the Society of Automotive Engineers.
- Adrian Pickering for his aid in manufacturing. His welding skill was a major asset to the completion of this project.
- The Society of Automotive Engineers club for their advice and willingness to help where needed throughout the project.
- All those who were able to donate financially to the project. They were a major aid in accomplishing our goal of having a fully functioning vehicle. Without them, we would not have had the means to complete this task. Their names are Charbrook Farm Nursery, Shore Sedghi, Christine Stimson, and Kevin Stimson.

Introduction

In the constantly evolving field of automotive engineering, researchers and designers continuously look to accomplish two tasks. They work to not only improve upon designs, but to also teach and inspire the next generation of engineers to take an interest in the challenges and rewards of automotive engineering. To aid them in their mission, a global association of approximately 128,000 engineers and technical experts was created, known as the Society of Automotive Engineers (SAE) International. The core values of SAE International are lifelong learning and voluntary consensus standards development.

SAE International hosts a large number of different collegiate events with two of the most popular being the Formula SAE and Baja SAE competitions. Both competitions engage students in real-world engineering design projects. The objective of the Baja SAE competition is to design an off-road vehicle capable of enduring the rough terrain. The competition is scored based on a number of aspects such as: design, challenge results, and a financial report.

The goal of this year's Major Qualifying Project (MQP) was to design a vehicle capable of withstanding the Baja SAE competition challenges. While the vehicle did not compete at this year's competition, it was the group's intention to have a functioning vehicle which can participate in the 2017 competition. For competition, all teams are provided with the same ten-horsepower Briggs and Stratton Intek Model 20 engine. Our group focused on a partial re-design of the chassis, suspension, steering, and drivetrain. In an effort to remain within the allotted budget while also creating a working vehicle, the group aimed to recycle as much of the vehicle as possible. Rather than purchasing all new parts, parts that were either available in storage or from the 2014-2015 vehicle were used or modified when possible. Design and development of this vehicle was completed through the use of various computer programs including, but not limited to: SolidWorks, MathCad, Matlab, and PMKS. Our group was provided with a variety of previous files for the vehicle; however, file corruption caused many SolidWorks assemblies to not open properly. Therefore, several parts needed to be remodeled.

In order to successfully complete this MQP, collaboration with several groups played an integral role. These groups included our advisor, sponsors, industry experts, and the Worcester Polytechnic Institute (WPI) SAE Chapter. These groups provided us with a significant pool of knowledge and advice that assisted the group in assembling a working vehicle. This vehicle will be used in the 2016-2017 Baja SAE competition and will create an environment for WPI SAE members to demonstrate the important engineering principles that they have learned. Since the vehicle will also remain part of the WPI SAE Chapter's property, it can be used to mentor new members and help them explore the field of automotive engineering.

Background

Components of a Baja Vehicle

Automotive vehicles in general and Baja vehicles more specifically, utilize many on-board systems that allow the vehicle to operate fully. These systems include the steering, suspension, brakes, engine, drivetrain, and frame. Vehicles also may utilize a variety of sensors in order to gather data about the vehicle and environment during use. For the purpose of this Baja vehicle, no sensors will be used in order to reduce complexity, the potential for failure of components, and vehicle weight.

Steering System

A vehicle's steering system comprises of several parts working together to create an optimal path for the tires to follow. This takes into account factors such as the angle at which the tires are contacting the surface of the ground and at what angle a tire's turning is being controlled from. Starting from the farthest point from the chassis, a vehicle's turning is dependent on the camber, castor, and kingpin inclination angle of the tires. The vertical alignment and angle of a tire compared to the vertical axis of suspension is what defines the camber. Due to this, it is possible for a tire to either have positive or negative camber (Riley, 2005).

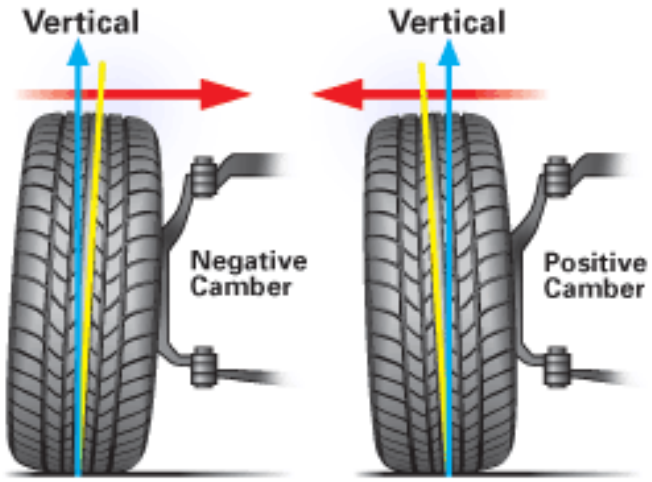

Figure 1: Visual Representation of Camber

As seen in Figure 1**,** when a tire is angled so that the top of the tire is towards the vehicle, negative camber is present. When a tire is angled so that the top of the tire is away from the vehicle, there is positive camber. While both types of camber have their benefits, negative camber is generally preferred among Baja vehicles. Positive camber offers a high risk of rollover in off-road situations and is unstable in high speed situations, whereas negative camber provides added off-road stability and allows for more contact between the tire and surface. Additionally, negative camber creates a camber thrust which helps to reduce lateral movement and tire scrubbing (Riley, 2005). This improves stability and control.

A second variable that is taken into account when working on steering is caster. Caster is viewed by drawing a line through the upper and lower ball joints and comparing it to the true vertical of the wheel. The orientations needed in order to achieve either positive or negative caster are shown in Figure 2.

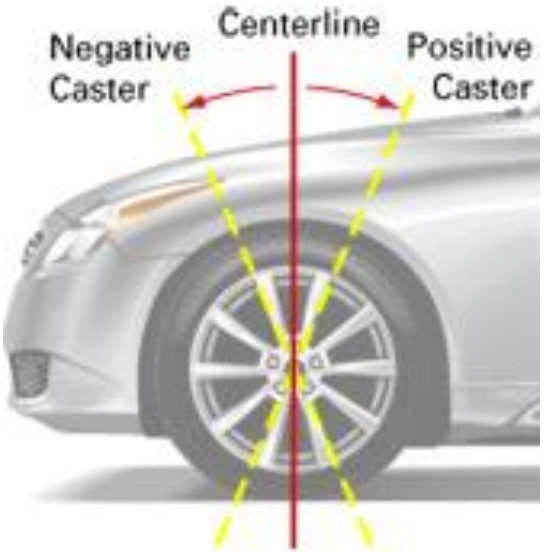

Figure 2: Visual Representation of Caster

Caster is important when taking stability at high speeds into account by creating a self-centering force (Riley, 2005). Additionally, caster helps to improve a car's front end cornering effectiveness and steering effort. Another way to visualize caster is to imagine a Harley-Davidson motorcycle and its steering forks. The steering forks form a positive slope between their top connection point and where they connect to the front wheel. This leads to the motorcycle having positive caster.

Vehicles also use a feature known as Steering Axis Inclination (SAI). The SAI is the angle between a vehicle's upper and lower steering pivot points and a vertical line drawn perpendicular to the ground. This can be seen in Figure 3. SAI increases a vehicle's straight-line stability and steering feel by making the axle travel in an arc while turning. This change in "steering feel" is created by the reduction in directional disturbances caused by obstacles. While eliminating the steering input of obstacles; however, the "feel" of the road is also lost (Riley, 2005).

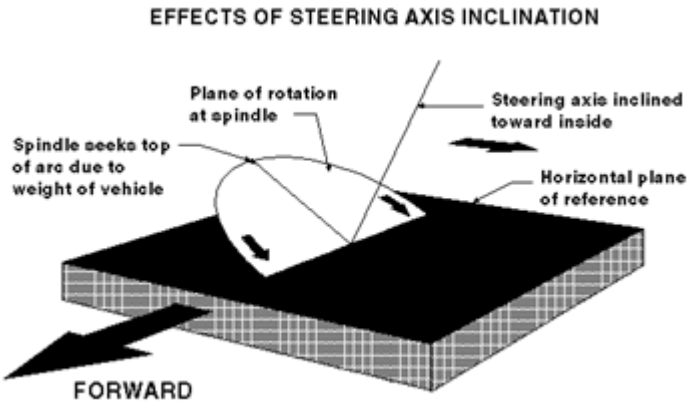

Figure 3: Visual Representation of SAI

Lastly, Ackerman steering is also utilized when designing the steering system of a vehicle. The issue when turning a vehicle is that one tire needs to travel a smaller turn radius than the other, which is impossible if they both are attempting to follow the same turn radius. In order to correct this issue, Ackerman steering must be used which allows for the inner wheel to have a sharper angle while the outer tire has a shallower angle (Thomsen, 2015). Ideally, a 100% Ackerman is desired which should result in no slip angle. To clarify, the slip angle does not mean that the tire is slipping or sliding. Slip angle refers to the flexing and/or twisting of a tire's contact patch during turning. In order to achieve 100% Ackerman, the turning center of all four tires must be the same as seen in Figure 4.

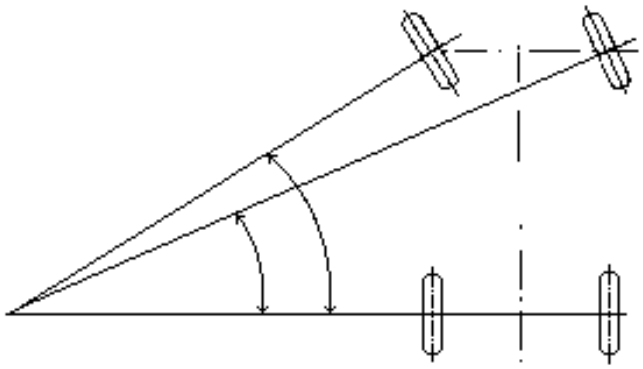

Figure 4: Ackerman Steering Principle

As seen in Figure 4, the outer tire must have a shallower angle than the inner tire in order to accomplish 100% Ackerman. To create this difference in angle, the steering arms must be simply mounted at the correct angles. This mounting option is shown in Figure 5, where the necessary angle to calculate and mount the steering arms at is alpha (α).

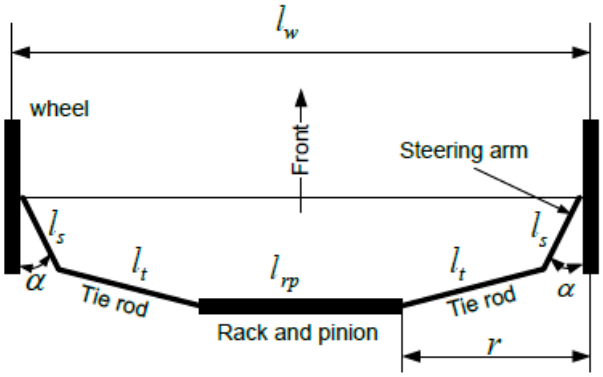

Figure 5: Diagram of Steering Angle

In Figure 5, l_w represents the width of the wheel base, l_s represents the length of the steering arm, l_t represents the length of the tie rod, α represents the angle between the wheel and the steering arm, r is the distance between the end of the rack and pinion and the wheel, and l_{rp} is the length of the rack and pinion.

Suspension

The suspension of a vehicle is critical to both safety and performance. The first and foremost duty of the suspension is to dampen and absorb the vertical forces that a vehicle might experience during use. This can include a small shift in weight when the vehicle is loaded with people or items to a large shift if the vehicle's tires run into a large obstacle on the ground. By dampening the vertical forces in these situations, the suspension protects both the vehicle and passengers from unwanted and potentially harmful vertical forces. Suspensions also perform two other basic functions. The first is known as ride height and the second is handling. The ride height of a vehicle refers to the quantity of vertical forces that a suspension system will effectively be able to negate as well as how comfortable the ride will be for the driver. The handling refers to how well the vehicle can be controlled during turning, braking, and accelerating by keeping all four wheels in contact with the ground (Dixon, 2009).

Suspension systems can utilize two main types of force dampening. The first is the use of springs such as coil-over springs, leaf springs, and torsion bars combined with a piston to provide fluid friction damping. The second is the use of oil and nitrogen in various valves contained in a fluid shock. Both system types revolve around the same concept of compression and decompression. In the field of SAE Baja competitions, teams generally rely on two of the aforementioned systems due to cost, reliability, adaptability, and weight. These two systems are the coil-over spring systems and the air-shock systems.

A coil-over spring system, as seen in Figure 6, consists of a coil spring which encases a shock absorber within it. This system functions by having the spring compress as the vehicle impacts an obstacle and then decompress to resume normal function. By compressing and decompressing, the suspension is able to transform the kinetic energy of the impact into potential energy. However, this only describes the use and role of the coil-over spring. The role of the

shock-absorber is to regulate the oscillation of the spring and prevent the spring from oscillating until all the absorbed energy has been released (Burger et. al, 2001). Although coil-over shocks are heavier and less adjustable, they are more durable and less expensive.

Figure 6: Coil-Over Shock (Left) versus an Air-Shock (Right)

Air-shock systems act similarly but are designed differently than coil-over shocks. In an air-shock system there is a sealed air cylinder with a rod inside, as also seen in Figure 6. The overall system is controlled by the presence of hydraulic oil and nitrogen. As a vehicle impacts an obstacle, the oil is displaced and causes the piston to press against the Nitrogen. This compresses the gas, which then expands to cause the shock system to rebound. The oil and Nitrogen then expand back to their normal operating pressures as the shock slowly stops oscillating. Nitrogen alters the height of the shock while the compression and decompression of the shock is controlled by the oil (Erjavec et.al, 2015). Air-shocks have many benefits and deficits when compared to coil-over shocks. They are generally more lightweight and are more adjustable; however, are less durable and more expensive and rebound slower.

Based on the research of previous years, it was found that a set of criteria would be the most effective way to decide between coil-over shocks and air shocks. These criterion included functionality, adjustability, damping characteristics, and spring load. With regards to functionality and adjustability, air shocks have a clear advantage. Air shock systems are extremely easy to adjust while coil-over shocks require a special tool and have little variation in their adjustments. Moving into damping characteristics, it is important to examine the potential obstacles that a Baja vehicle may encounter during a competition. For this reason, it was important to view which shock system would allow for a quicker rebound to obstacles while also remaining easy to adjust. However, both systems are able to fulfill both halves of this criterion (Crevoiserat et.al, 2015). Lastly, the load that both air shocks and coil-over shocks can support was examined. Given data from the previous year's MQP team, it was found that the vehicle would weigh roughly 600lbs fully loaded. The team assumed a 40% weight distribution in the front and 60% weight distribution in the rear which led to approximately 240 lbs and 360 lbs in the front and rear, respectively (Atamer et.al, 2014). After examining several purchasing options, it was decided that coil-over shocks would be the best option based off the aforementioned

criteria and cost. The cost of each shock option can be seen in Appendix B based off the 2014-2015 MQP team's data. Polaris RZR 570 shocks were purchased through a Baja sponsorship program. The loads capable of being supported by the front and rear springs were 115 lbf/in and 185 lbf/in, respectively (Crevoiserat et.al, 2015).

Control Arms

A vehicle's control arms are one of its simplest and yet most important components. They hold the knuckles, spindles, and axles firmly onto the car while controlling the geometric movement of the suspension. Vehicles also feature one of two types of suspension. The first type of suspension is dependent suspension. In this suspension system, the movement of one wheel is transferred to the other wheel via a rigid beam. This is generally used in the rear of cars that are meant for paved roads as well as the front of heavy trucks. Dependent suspension systems are used for leaf spring suspensions, Panhard rod suspensions, and Watt's linkage suspensions (Vivekanandan et.al, 2014).

The second type of suspension is independent suspension. Independent suspension systems embody exactly what their name implies; the movement of each wheel is independent of the other. This system is more widely used in passenger cars and light trucks since they provide more room for assemblies such as the engine and are more resistant to steering vibrations. Swing axle suspensions, Macpherson strut suspensions, double wishbone suspensions, trailing arm suspensions, semi-trailing arm suspensions, and transverse leaf spring suspensions are all forms of independent suspension (Vivekanandan et.al, 2014).

It had been found that independent suspension would be more desired than dependent suspension due to the adjustability of each suspension system, especially in an off-road environment. Within these system types, the most suitable suspension types for a Baja vehicle were the Macpherson strut, double wishbone, trailing arm, and semi-trailing arm suspensions. This decision was based off a variety of factors such as cost, handling capabilities, and deflection that each suspension could support (Crevoiserat, et.al, 2015).

Macpherson struts and double wishbone suspensions are generally used in the front of the vehicle. In a Macpherson strut suspension system, the spindle of the wheel is attached to a structure similar to a lower a-arm. This structure secures the bottom of the spindle while the top is connected directly to a coil-over spring which serves as the upper a-arm. Together, these form the connection points for the spindle and serve as the kingpin axis. The Macpherson strut has several benefits including a simple design, low cost, lightweight, and efficient packaging. A disadvantage of this system is that is has a relatively fixed camber which cannot be adjusted as easily as other systems (Riley, 2005). Macpherson strut suspensions are also more commonly used on vehicles with low or limited suspension travel for this reason which makes it a non-viable option for a Baja vehicle that is expected to have a large amount of suspension travel. A closer look at a MacPherson strut can be found in Figure 7.

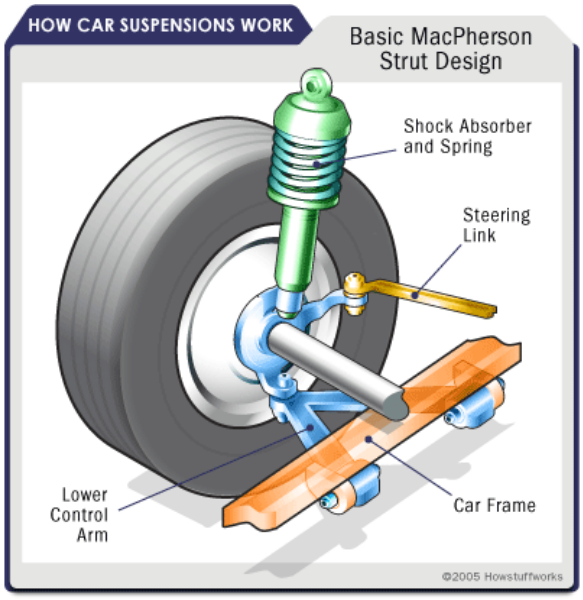

Figure 7: Macpherson Strut

Double wishbone (or A-arm) suspension systems utilize two lateral control arms which are typically unequal in length and connected to the spindle with two ball joints located at the upper and lower A-arm spindle mount locations. By allowing one A-arm to be shorter than the other, it is easy to induce a camber in the wheel. In this case, shortening the upper A-arm and decreasing the vertical distance between the upper and lower A-arm chassis mount points induces a negative camber thus improving stability and control. Overall this can improve a vehicle's dynamic characteristics and ability to handle larger vertical loads (Vivekanandan et.al, 2014). Another benefit of the double wishbone suspension system is that it allows the designer of the vehicle to place the reaction point of the wheel at almost any point in space. This system does have its disadvantages which include higher weight, higher cost, and more complex components (Riley, 2005). A visual representation of a double wishbone suspension can be found in Figure 8 below.

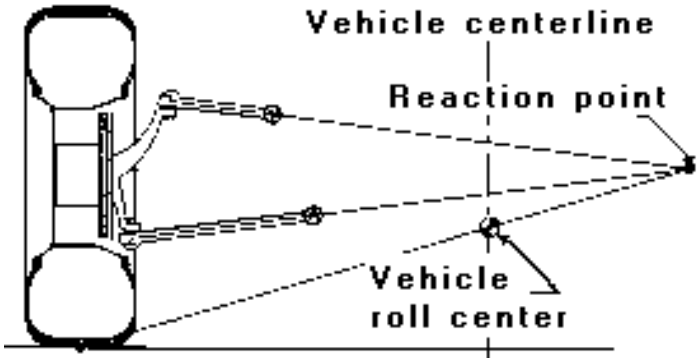

Figure 8: Double Wishbone Suspension

Trailing and semi-trailing control arms are generally found in the back of a vehicle. They are essentially the same with regards to design and function; however, trailing arms are mounted perpendicular to the vehicle's centerline while semi-trailing arms are mounted at a slight angle. Trailing arms allow wheels to move up and down over any bump, but restrict the ability for lateral movement and camber change. Due to this, manufacturers and designers lean towards the use of semi-trailing arms which function by utilizing a transverse component and trailing component shown in Figure 9. By using these two components, semi-trailing arms feature a camber which changes throughout suspension travel. For this reason and the ride quality associated with semi-trailing arms, a double wishbone suspension is more desired (Wan, 2000).

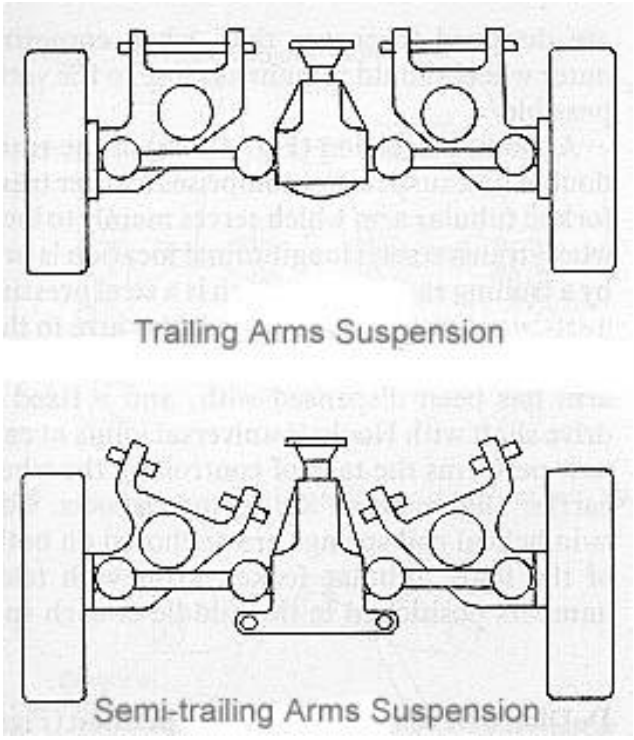

Figure 9: Trailing and Semi-Trailing Arm Suspension

Overall, a double wishbone suspension was chosen as the suspension system for all four wheels. The double wishbone suspension would provide greater steering assistance, more camber effect, better handling, and more adjustability versus a Macpherson strut and semi-trailing arm, making the double wishbone the ideal suspension type (Crevoiserat et.al, 2015).

Brakes

Brakes are one of the most important components of a vehicle with regards to accident avoidance and must function under all possible operating conditions including various road conditions, wear conditions, weight of the vehicle, and driver experience. Brake systems must accomplish three primary tasks which are slowing and/or stopping, maintaining speed on a downgrade, and holding stationary on a downgrade (Limpert, 2011).

Brake systems are available in two main styles. The first is drum brakes and the second is disk brakes. While both systems are designed using similar principles to dissipate kinetic energy through conversion to thermal energy, they function quite differently. Drum brakes are generally used on medium to heavy duty trucks across the world while disk brakes are utilized on most passenger vehicles. The reason that disk brakes are more sought after for applications similar to that of a SAE Baja vehicle is that they are far less sensitive to temperature spikes during braking. See Figure 10 for a description of disk brakes. Disk brakes can operate with little fade at high temperatures that reach approximately 1073 K to 1173 K. This is caused by the expansion of the brake rotor as heat builds up which causes no loss in brake fluid. In contrast to this, drum brakes can only operate up to approximately 673 K to 700 K before damage may occur (Limpert, 2011).

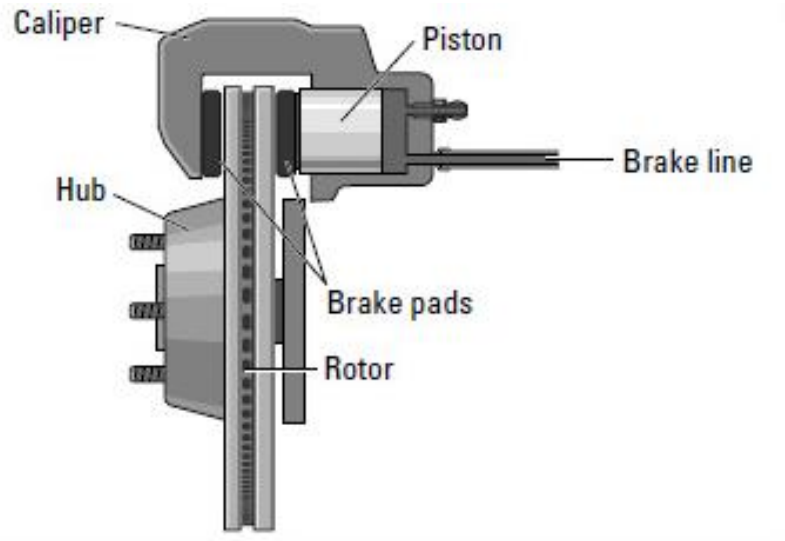

Figure 10: Floating Caliper Disk Brake

Disk brakes were selected by the 2014-2015 MQP team due to their ability to maintain brake effectiveness at high temperatures. With the possibility for repetitive braking during a competition and potential for quick braking, the brake systems may experience sudden peaks in

temperature. Additionally, due to their easier assembly and servicing, disk brakes are a far more desirable option for the application of an SAE Baja competition (Crevoiserat et.al, 2015).

Engine and Drivetrain

Each SAE Baja team is provided with the same Overhead Valve (OHV) Intek Model 20, 10-horsepower engine. This four cycle, air cooled engine by Briggs & Stratton provides 305cc of displacement with a 2.438 inch stroke and 8.0 to 1 compression ratio (Briggs and Stratton, 2015). However, this engine alone cannot power a Baja SAE vehicle through the many challenges that Baja SAE competitions offer.

In order to increase the output obtained from the engine without modifying the engine, a Continuously Variable Transmission (CVT) must be used. A CVT transmits power from the engine to the wheels by changing the diameter of the CVT cones. It can also adjust a vehicle's engine's torque in an infinite number of ways. This makes a CVT far more efficient that a normal gearbox. By properly tuning of the CVT, it is possible to improve the vehicle's power output while ensuring that the vehicle is still fuel efficient. (Rahman et.al, 2013). Additionally, since a CVT functions similarly to an automatic transmission, no pneumatic clutch is required in this system since it is powered by a torque converter. CVT's are desirable in this situation because they have a large range of transmission ratios, are lightweight, easy to tune, and have models that were specifically produced for mini-Baja applications.

There are three types of throttle cables used in combination with the Model 20 engines. The first type is a basic bike cable. The basic bike cable is covered, cheap, light, and easy to modify. For this reason, many teams opt to use this cable. A second cable type is the push/pull cable. The push/pull cable is very similar to the basic bike cable; however, instead of having cable extending from each side of the covered regions, it is completely sealed and uses linear sliders to achieve the motion that can be observed. Push/pull cables are much more durable than basic bike cables, but are less modifiable due to its thickness and complete seal. Lastly, there is a throttle cable which is a preassembled kit that must be purchased to the correct length. The drawbacks of this cable system are that it is far more expensive than the other two and can cause issues if a proper length cannot be found. Due to the previously existing partnership with Polaris after the purchasing of the RZR 570 coil-over shocks, a Polaris push/pull cable was purchased and fitted to the vehicle (Crevoiserat et.al, 2015).

Methodology and Procedures

Suspension and Steering

Camber

After examining the positive effects of negative camber gain throughout suspension travel, it was decided to utilize a negative camber of no more than 6 degrees at full shock compression. This was determined by researching the optimal amount of negative camber that

should be used in an off-road racing environment along with examining the camber utilized by other teams. Recent teams at WPI have performed their calculations and found that the camber should be below 7 degrees (Boyle et.al, 2013). In order to determine the currently existing camber based off the unmodified frame, the double control arm system needed to be measured and modeled for simulation. The modeling for the control arms, shown in Figure 11, was done with PMKS software.

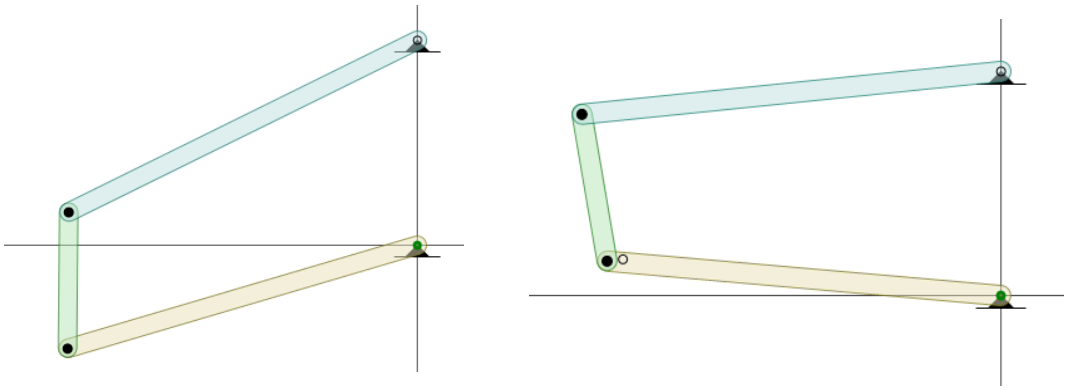

Figure 11: PMKS Model of Control Arms

Using measured lengths, an angle finder, the shock mounted between its chassis location and lower A-arm location, and the pin joint locations of the A-arm chassis mounts law of cosines, the starting angles of the original upper and lower control arms were able to be determined. These values were found to be approximately -35 degrees and -30 degrees respectively. Utilizing the graphical analysis approach and PMKS simulation, the kinematic relationship of the upper and lower A-arms with respect to the spindle demonstrated a 10 degree change in camber throughout suspension travel. Due to the geometry of the front suspension, this 10 degree change in camber flows incorrectly toward 10 degrees of positive camber at full suspension compression. After allowing the linkage to fully rotate in the PMKS simulation, the data was downloaded in a text format. All the angle values created by the spindle as the control arms traveled through their full range of motion were then determined from the PMKS data. The law of cosines was used with a measured value of the length of the fully compressed coil-over shock. This confirmed the previous calculations and found that the control arms can only rotate for a total travel of 34 degrees. Returning to the PMKS text data, all values of control arm rotation that were beyond 34 degrees were removed. This limited the remaining spindle angle values to only the possible angles given the vehicle's configuration. Analysis of the previous front suspension verified that there was a need for upper A-arm chassis mount relocation.

Front Control Arms

One of the initial steps of building this year's vehicle was to remove the four-wheel drive. The four-wheel drive was removed for a variety of reasons. First, the interaction of the four-wheel drive spindle with the A-arms caused the front rims to significantly rub against the A-arms when turning. Additionally, in order for the four-wheel drive spindles to properly seat within the rims, part of the spindle was ground down by the previous MQP group reflecting poor manufacturing practice. Finally, the four-wheel drive system composed of a long drive shaft, two half shafts, and a front T-box differential added weight to an already heavy and power limited vehicle. It was decided that the added traction created by a four-wheel drive system did not exceed all of the issues that it created. The team also decided that the spindles from the previous MQP should not be reused for this year's Baja vehicle. The previous MQP's spindles were not used because they were designed for 4 wheel drive adding a significant amount of unnecessary weight of nearly 20 lbs a piece. The original spindles required the use of hub adapters which would have needed to be manufactured in order for the hubs to fit the 4x110mm bolt pattern on the front rims.. Previous years had purchased free spinning hub assemblies that were still in their packaging and significant discussion occurred weighing the possibility of using these smaller and lighter hub assemblies seen in Figure 12.

Figure 12: Front Wheel Hub Assembly

The issue with the spindle and hub assembly in Figure 12 was that it was much smaller than the four-wheel drive spindle and hub assemblies. When doing camber calculations and kinematic analysis, the effective spindle length for the new spindles was about 2.0 inches shorter than the ones in use by last year's group. This created a major issue with the four bar linkage geometry due to the way that the double A-arm configuration works. Previously stated, the kinematic relationship between the previous front suspension setup yielded an incorrect positive

camber at full compression and replacing the spindle with a much shorter spindle exaggerates positive camber even further.

Additionally, the in-stock spindle and hub assembly was designed for a Macpherson strut suspension which would have caused a full suspension redesign and the use of a non-optimal suspension for Baja application. A major decision was made early on to salvage as much of the previous car as possible and making the double A-arm suspension work effectively was a top priority. There were several factors that influenced this decision such as time, manufacturing, and cost restrictions; however, one of the strongest points to remain with the present design was the necessity to prevent the camber from surpassing 6 degrees of negative camber. Using a Macpherson strut would have created many issues due to the presence of a fixed camber over the entire travel of the control arm. If truly considered, given 34 degrees of suspension travel with an initial state of 0 degrees with respect to the "y" axis, the negative camber at full suspension compression would be -34 degrees.

In order to create proper camber geometry, several solutions were created. The first solution, as suggested earlier, was to simply create a new upper A-arm crossbar mount on both sides of the front of the vehicle, seen in Figure 13. This would allow for the kinematic relationship between the initial four bar suspension linkage to be corrected to reflect a negative camber trajectory. This looks like a functioning solution when the shock is not taken into account. With the addition of a shock into the assembly, there is a high risk for collision between the shock and control arms.

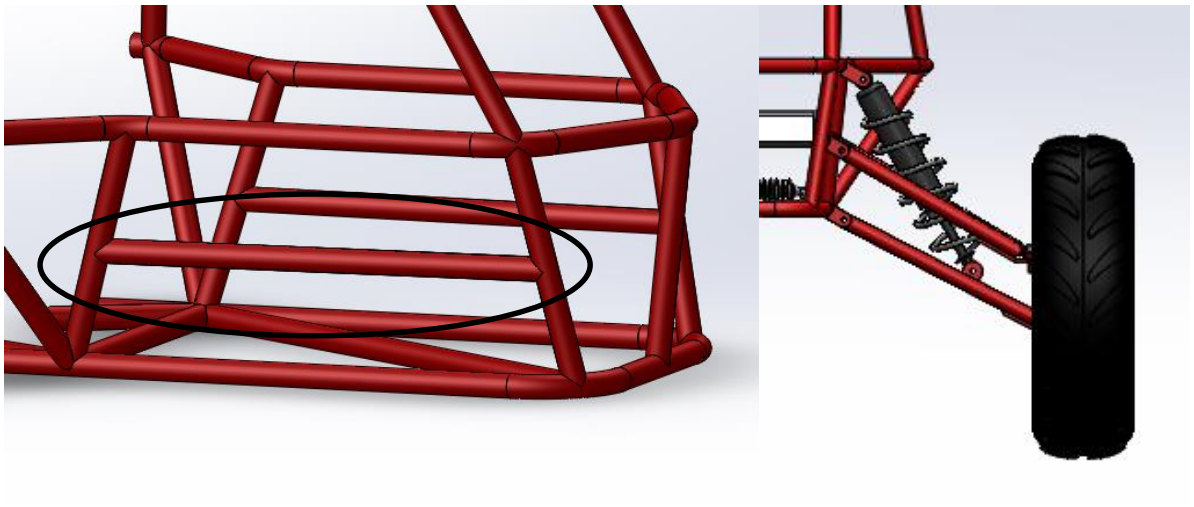

Figure 13: Control Arm Solution 1

In an effort to produce a lightweight spindle, a custom knuckle was designed. Figure 14 shows the design of the custom knuckle. This design combined the dimensions and design of the four-wheel drive spindle without the weight of the female spline. The new design would utilize the brakes and hubs from the previous MQP and would eliminate the gap created by using smaller spindle and hub assemblies. This spindle would be manufactured out of forged steel,

similar to many other spindles used in the automotive industry. Due to manufacturing challenges, cost, and lead time concerns with outsourcing, the idea was not accepted.

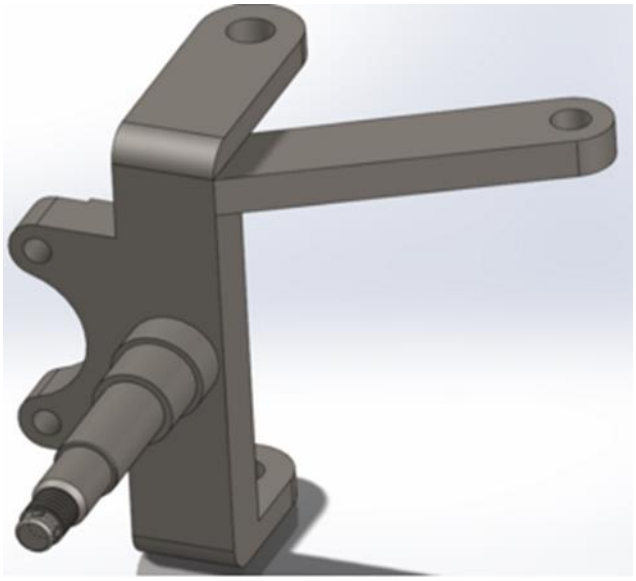

Figure 14: Custom Knuckle Design

The final solution to bridge the spindle gap between the upper and lower A-arms was to purchase off the shelf parts. The group wanted to find a larger spindle and hub assembly that would not only meet the size requirement to satisfy the geometry of the control arms but also to fit the bolt pattern of the rims. No such spindle exists. The spindle size to satisfy the suspension kinematics is simply too large for any manufacturer to have created. A set of spindles and hub assemblies that came off a 2004 Kawasaki KFX-400 four-wheeler were found at a local cycle salvage shop and were slightly smaller than the current four-wheel drive spindles. A CAD

model of the spindle can be seen in Figure 15. The new KFX-400 spindles are shown Figure 16 and Figure 17.

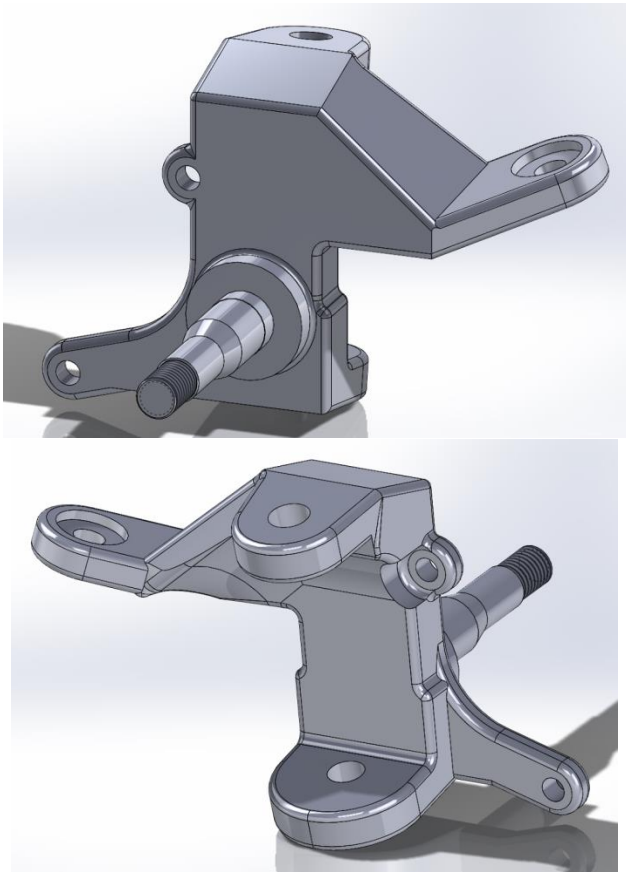

Figure 15: CAD Model of KFX-400 Spindle

Figure 16: 2004 KFX-400 Spindle

Figure 17: 2004 KFX-400 Spindle

Additionally, the purchased hubs also fit our 4x110mm lug pattern rims, as shown in Figure 20, Figure 21, Figure 18 and Figure 19

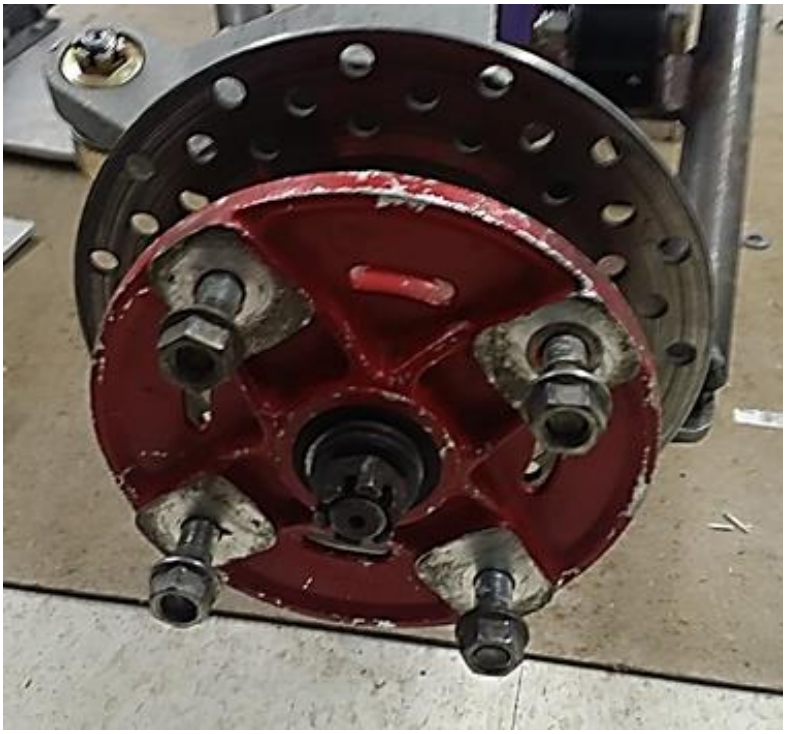

Figure 18: 2004 KFX-2004 Hub

Figure 19: 2004 KFX-400 Hub Assembly

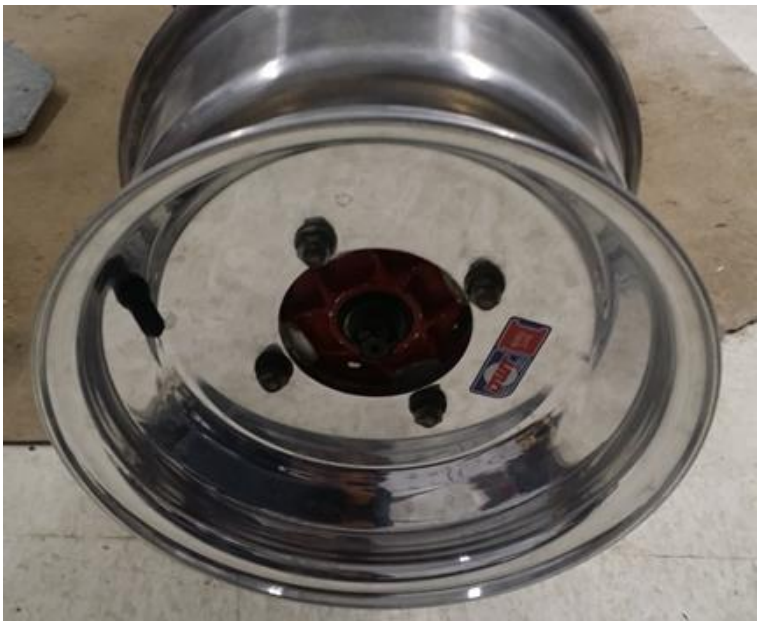

Figure 20: 2004 KFX-400 Hub Assembly Mounted to Rim

Figure 21: 2004 KFX-400 Hub Assembly Mounted to Rim

There were many unknowns within the needed suspension redesign so the use of simulation software was not a feasible option to figure out all dimensional and relocation modifications needed to ensure correct camber. It was necessary to trace out as much of the known factors to try to methodically solve the kinematic geometry as a whole. Through

graphical analysis, the KFX-400 spindle was found to work within the original front double A-arm suspension with a few suspension modifications. As discussed earlier, moving the upper A-arm chassis mount points down would allow the team to reach the goal of -6 degrees of negative camber at full shock compression.

Research was performed on common double A-arm link lengths coupled with spindle height and vertical distance between chassis mounts. The only valuable insight gathered was that double A-arm suspensions tend to utilize a shorter upper A-arm than the lower and the vertical distance between the upper and lower A-arm chassis mounts is always smaller than the spindle height in order to produce proper camber. The only true initial known geometric values were lower A-arm length and its initial position along with the KFX-400 spindle height and its initial orientation.

With consideration of the shock chassis mount and where it connects to the lower A-arm, it was easy to trace out the initial position of the lower A-arm with respect to the chassis. The distance between the lower A-arm chassis mount and shock chassis mounts must be plotted for initial reference. Both mounts serve as compass pivot points. Once the lower A-arm was drawn in its initial state, the spindle was drawn off of where it would be mounted to the lower ball joint in its 0 degree orientation. The front shock compresses a total of 5.2 inches and its compressed rotation about its chassis mount was drawn using a compass. Knowing that the lower A-arm must rotate about its own chassis pivot point and the position of the shock mount on the lower A-arm, a path can be traced from the shock mount on the lower A-arm until it intersects with the fully compressing shock arc. This intersection reflects the complete travel of the lower A-arm. The complete lower A-arm was then translated to reflect its orientation when the shock is fully compressed. As previously explained, ideal camber at full suspension compression is -6 degrees. The spindle can then be traced to reflect -6 degrees of camber at full shock compression. Given the upper ball joint mounting points of the spindle at initial position and at its translated fully compressed shock position, the midpoint of the vertical distance can be translated along the “x” axis till it is in line with where the new upper A-arm chassis cross mount tube should be welded in. This position is represented by the Chassis tube centerline in Figure 22. Since the upper A-arm chassis mount dimensions were known due to early purchase, an arc was traced about the midpoint plotted on the chassis tube centerline to represent all possible chassis mount position angles. After finding the ideal upper A-arm chassis mount angle, a visual representation of the original upper A-arm was traced. By taking the common length that joins both upper ball joint positions in one arc, the necessary cut length was able to be marked. Throughout this long procedure, the precise suspension modifications could be made to correct the camber trajectory throughout complete suspension travel. Refer to Figure 22 for a visual representation of this procedure.

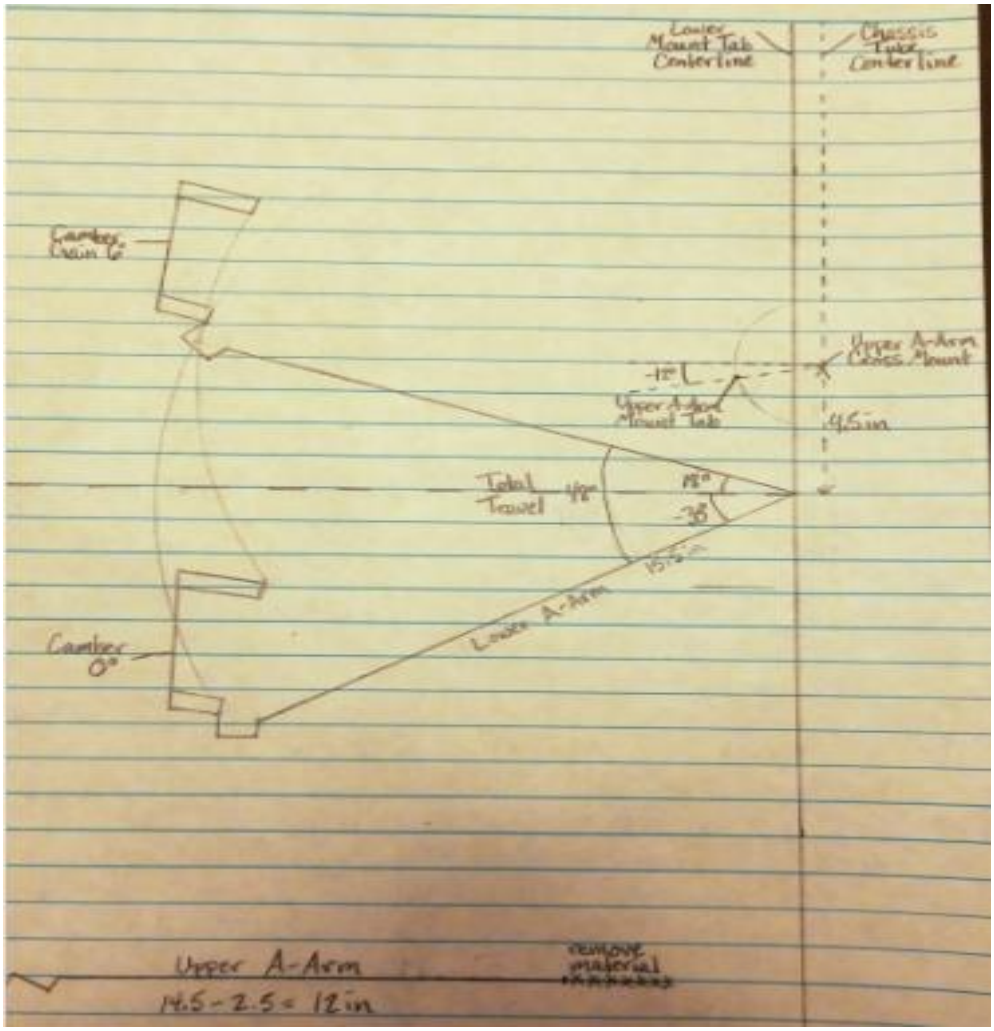

Figure 22: Graphical Analysis

After figuring out the changes necessary to correct the front suspension, 4130 Chromoly tubing was purchased to be cut and welded to the chassis to relocate the upper A-arm cross mounts. Using the drill press with a hole saw jig, the proper fish mouth cuts were able to be made to insure tight fit of the cross mount tubes to the chassis for welding. The upper A-arms were cut down using an angle grinder with a circular cutting blade and previously purchased tubing with 1.125 inch diameter by .058 inch wall thickness was used to sleeve the two cut pieces to provide stability and two areas of circumference welds. The purchased upper A-arm chassis mount tabs were then mocked up, traced and welded to the chassis. In Figure 23, the finished front suspension is represented.

Figure 23: Completed Front Suspension

Tie Rods and Linkages

Due to all of the changes that have been made to the suspension and spindles, the tie-rods that were used by the previous MQP no longer work for our application. The swages from the last MQP were not large enough to handle the stresses that would be expected from a Baja competition; therefore, in an effort to limit the possibility of catastrophic failure, we decided to purchase new, stronger swages. Additionally, the swages from the previous MQP were of different length which resulted in the need to mount the steering rack off center of the frame, purchasing new swages will allow us to center the rack. Finally, the provided swages are not compatible with the new spindle that we purchased because it uses a different size screw to mount to the steering arm of the spindle. The different screw size would create slop in the connection between the swage and the steering arm which would drastically hurt steering performance.

Caster & Steering Axis Inclination

While caster and steering axis inclination both offer improvements in the area of handling and stability, they would be two aspects that we would not be able to alter. Given the time and budget constraints that exist within our project, it was found that it would not be a feasible task to re-design the front control arms and knuckles in order to obtain the slight benefits from using the proper caster and SAI angles.

Ackerman Steering

In order to utilize Ackerman steering and reduce the slip angle during turns, it was necessary to calculate the mounting angles for the steering arm angles. Using the following equation, we input measured values for the center to center distance between wheel pivots (t) and the wheelbase length (L).

$$\text{Steering Arm Angle} = \operatorname{atan}\left(\frac{t}{2 \cdot L}\right)$$

When calculated, it was found that the angle at which the steering arms must be mounted is 18.7 degrees. Mounting our steering arms at this angle would be an easy task given that the steering had not yet been mounted entirely in the vehicle. This allows us to mount our rack and

pinion wherever necessary to achieve the desired angles and near 100% Ackerman. Knowing several values regarding our steering mounting, we were able to calculate our Ackerman Percentage, Ackerman Factor, and Turn Radius.

$$Wheelbase\ (L) = 65in$$

$$Track\ Width\ (T) = 60in$$

$$Turn\ Angle_{max}\ (\alpha) = 30°$$

$$Turn\ Radius\ (R) = 65in \cdot \tan(60°) = 9.33ft$$

$$Ackerman\ Angle\ (d_{ack}) = \text{atan}\left(\frac{T}{R}\right) = 28.1°$$

$$Steering\ Arm\ Length\ (A) = 4in$$

$$Steering\ Arm\ Lateral\ Length\ (B) = 3.875in$$

$$Tie\ Rod\ Lateral\ Length\ (C) = 16.25in$$

$$Tie\ Rod\ Length\ (D) = 5.5in$$

$$Deriv1a = A = 4in$$

$$Deriv2a = -B = -3.875in$$

$$Deriv1b = -D \cdot \left(\frac{B}{C}\right) = -1.31$$

$$Deriv2b = D^2 \cdot \left(\frac{B^2}{C^3}\right) = 0.106$$

$$Deriv2c = -D \cdot \left(\frac{A}{C}\right) = -1.35$$

$$Deriv2d = \frac{-B^2}{C} = -0.924$$

$$f'(x) = Deriv1a + Deriv1b = 2.69$$

$$f"(x) = Deriv2a + Deriv2b + Deriv2c + Deriv2d = -6.043$$

$$Ackerman\ Factor\ (AF) = \frac{-2f"(0)}{f'(0)} = 4.49$$

$$Percent\ Ackerman = \frac{0.77\alpha_{w_i}}{d_{ack}} = 82\%$$

These calculations tell us a great deal about the maneuverability of our vehicle. With a calculated turn radius of approximately 9 feet, our vehicle should be able to compete with the maneuverability of many other vehicles. Additionally, with an Ackerman Percentage of 82%, we have made our steering close to 100% and should not experience a large amount of tire slip.

Steering Restrictions

The initial orientation of the KFX-400 spindle and hub assembly and the orientation of the A-arms with respect to the front rims showed the potential of rim to A-arm conflict during a fully turned steering situation. Since last year's group wanted to incorporate four wheel drive they had to stagger the shocks with the ball joints due to the need to run half shafts out to the front spindles. This stagger caused them to set the ball joints back slightly toward the rear of the vehicle instead of centering them on the A-arms which resulted in the front of the rims to rub when the wheel is turned toward the center of the vehicle. The best solution which avoids A-arm redesign was to introduce 1.25 inch wheel spacers that increase the track width of the car without exceeding Baja competition guidelines for maximum track width (64 inches). This solution allowed for more space between the rim and the A-arms and can be referred to in Figure 24 and Figure 25.

Figure 24: Side View of Wheel Spacer and Hub Assembly

Figure 25: Complete Tire, Wheel Spacer, and Hub Assembly

Steering Column Assembly and Mounting

The Steering Column posed multiple challenges within its design, assembly, and chassis mounting. Initially the steering rack and pinion was raised and angled in order to ensure the steering wheel would fall into the driver's hand at a comfortable angle. Through research, raising the rack and pinion is not ideal because in significantly affects bump steer which is the amount that the tires turn about the kingpin when encountering a large road undulation. Mounting the steering rack and pinion flat in the cockpit combined with an additional universal joint (U joint) allows raising the rack and pinion to be avoided. The second U-joint caused a need for more steering column to be purchased. The second U joint was referred to as a DD U joint due to its internal bore shape looking like two "D's" back to back. The DD U joint caused a need to manual mill flats into the steering column rod for proper fit within the bore. Set screws are located in the middle of each flat to prevent the steering column from sliding out of the DD bore. The first U joint had a misalignment maximum of 30 degrees while the second DD U joint had a maximum misalignment maximum of 50 degrees. Together a misalignment of 60 degrees was the resultant angle that the final portion of the steering column pointed. To prevent excessive wear on each U joint, each had an extra 10 degrees of play as suggested by the retailer and were mounted in parallel phase. Parallel phase is when each U joint yoke on either end of a shaft are in the same exact rotational orientation. An image of the assembled steering column is located in Figure 26

Figure 26: Double U Joint Steering Column Configuration

It was important to secure the steering column to the chassis to minimize extra steering play which has detrimental effects on handling. The steering column was mounted to the chassis using a cross mounted tube that was welded horizontally between the secondary upright tube chassis members. A tab was welded tangent to the cross mount tube directly in the center and was designed to house an oval flange bearing which fixes the steering column in space with set screws. An example of the finished product can be seen in Figure 27 and Figure 28.

Figure 27: Complete Mounted Steering Column

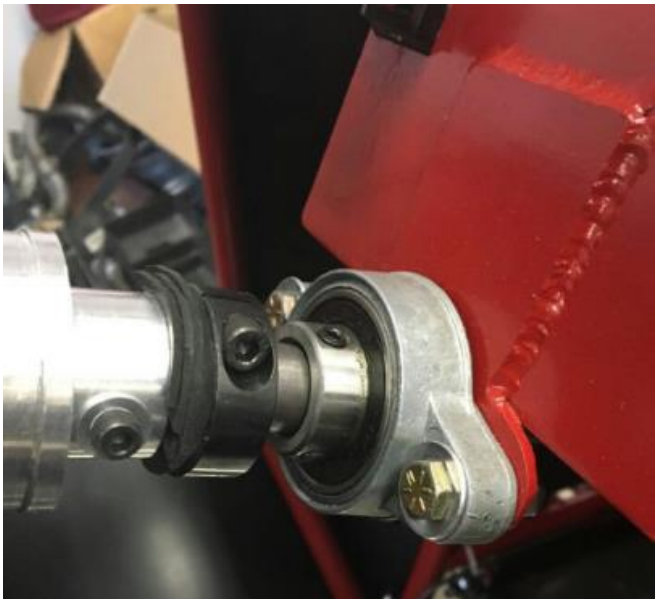

Figure 28: Close Up of Oval Flange Bearing Mounted to Chassis Tab

Rear Control Arms

The rear control arm design and orientation were another source of concern. A problem that existed with the frame was created by the angles of tube mounts present at the rear of the vehicle. A special control arm set needed to be manufactured to mount the rear wheels. This special control arm set was too large on the upper A-arm and allowed for some collision between the rim and control arm. To fix this the rear of the frame was redesigned. The redesigned frame, seen in Figure 29, created parallel support tubes in the rear of the vehicle. This allowed for easier

mounting and design of the control arms, and created additional room for the drivetrain. The modified rear also allowed for the shock to be properly mounted to the frame. Before, the only way to orient the shocks correctly was with excessively long mounting tabs which created a large moment about the mounting tabs. This was an exposed weakness due to the massive forces absorbed through the suspension system and the likelihood of significant deflection to occur. A local shop, Hubb Equipment, performed the welding for free, provided that the group paid for the necessary stock material. The results of the frame redesign are shown in Figure 30.

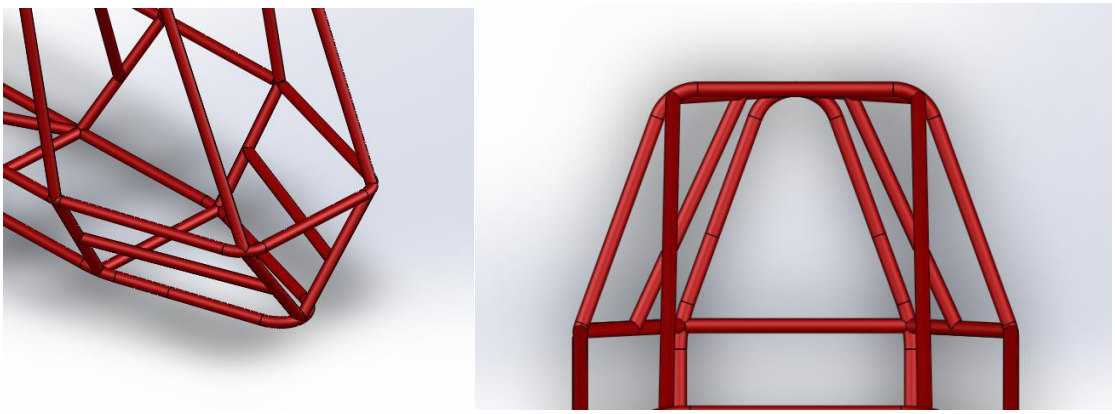

Figure 29: Redesigned Rear Frame

Figure 30: Actual Frame after Hubb Equipment Welding

It was decided to utilize the rear, lower control arms designed and manufactured by the previous MQP. This was a decision made primarily based on the time, monetary limitations, and the functionality of the A-arms. New rear, upper control arms needed to be designed and manufactured due to the frame redesign. Two designs were created. One design wrapped around the shock and another which angled towards the front of the vehicle and avoided the shock. The

later design was chosen to limit the chances of interference with the shock. The design is shown in Figure 31 and Figure 32.

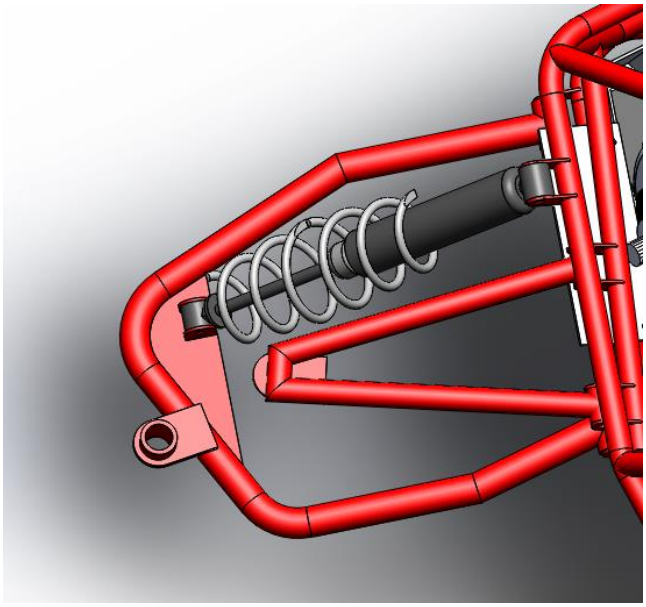

Figure 31: Redesigned Rear, Upper Control Arms

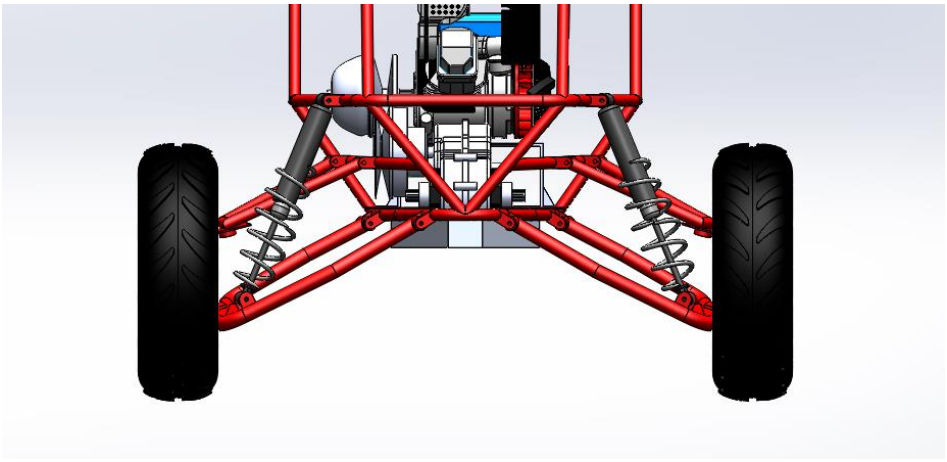

Figure 32: Redesigned Rear Control Arms

The design was then manufactured with 4130 alloy steel tubing. The tube was cut and mocked together before welding, see Figure 34. The bearings from the previous MQP were salvaged and used to attach the upper control arms to the tabs on the vehicle. The ball joints were removed from the old control arms as well and were re-welded to the new control arms. Next,

0.375-inch steel tabs were welded to the control arms for the attachment of 10-inch tie rods. The tie rods were used to prevent the wheels from turning and to properly align the wheels.

Figure 34: Finalized Rear Suspension

Mechatronic Analysis of Suspension

After the design of the suspension was completed, a mechatronic analysis of the system was conducted. Bond graph methods were used to derive equations of motion. To simplify the analysis, a half car model was used to model the vehicle; one side of the vehicle was used viewing both the front and rear suspension.

The expected dynamic response is the rotation of all members. The upper A-arm is expected to rotate about its axis. When it rotates upward, the spindle will rotate, exhibiting a slight degree of negative camber. Also, the lower A-arm will rotate upward as well. Since the shock was mounted to both the chassis and lower A-arm, it will also experience an angular velocity. All of these motions contribute to the section of the suspension allowing the wheel to move up and down and allowing the chassis to undergo less stress when going over obstacles.

Planar motion was utilized for the representation of each individual shock because of how vital camber is to this system. The vehicle will be moving up and down relative to the ground and the tires will experience the same undulation. Therefore, planar motion was needed to model this system accurately. As seen in the free body diagrams shown in Diagram 1 and Diagram 2 of Figure 35, different nomenclature was used to model the front and rear suspensions. They each played a role in how the entire vehicle reacts to road undulations. Diagram 3 of Figure 35 shows a simplified version of the entire system in that light. Also, taking into account the weight of the vehicle, the center of mass was assumed to be 2/3 from the front of the vehicle. This is shown in Diagram 4 of Figure 35.

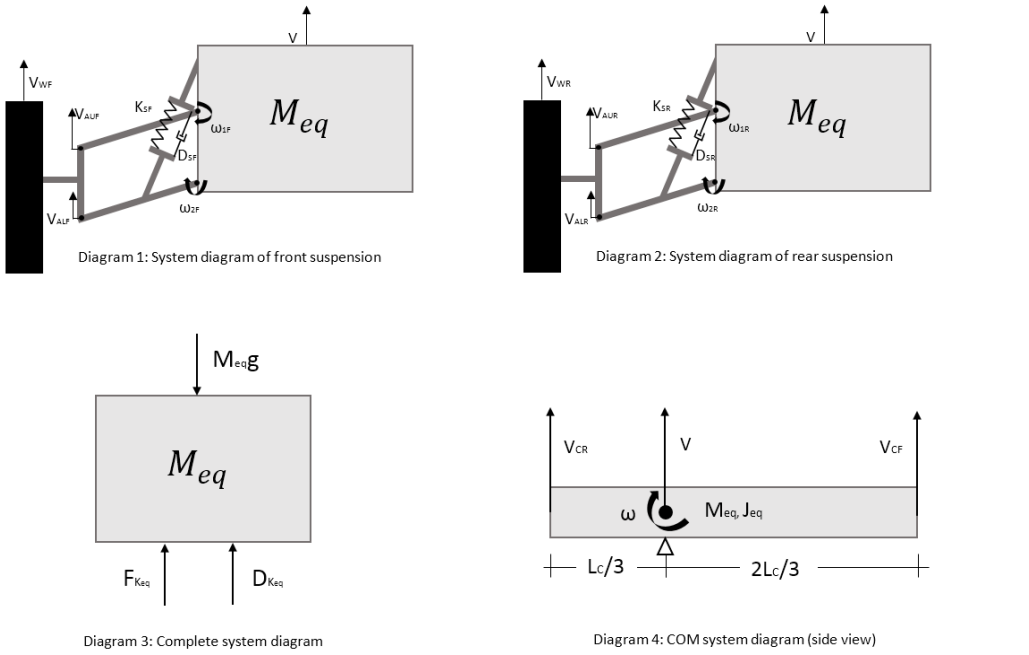

Figure 35: Free Body Diagrams of Half Car Model

From the free body diagrams, the bond graphs in Figure 36 were derived. The left side of the graph shows the front of the vehicle and the right side shows the rear of the vehicle. The center of the graph depicts how the suspensions work with the center of mass of the vehicle.

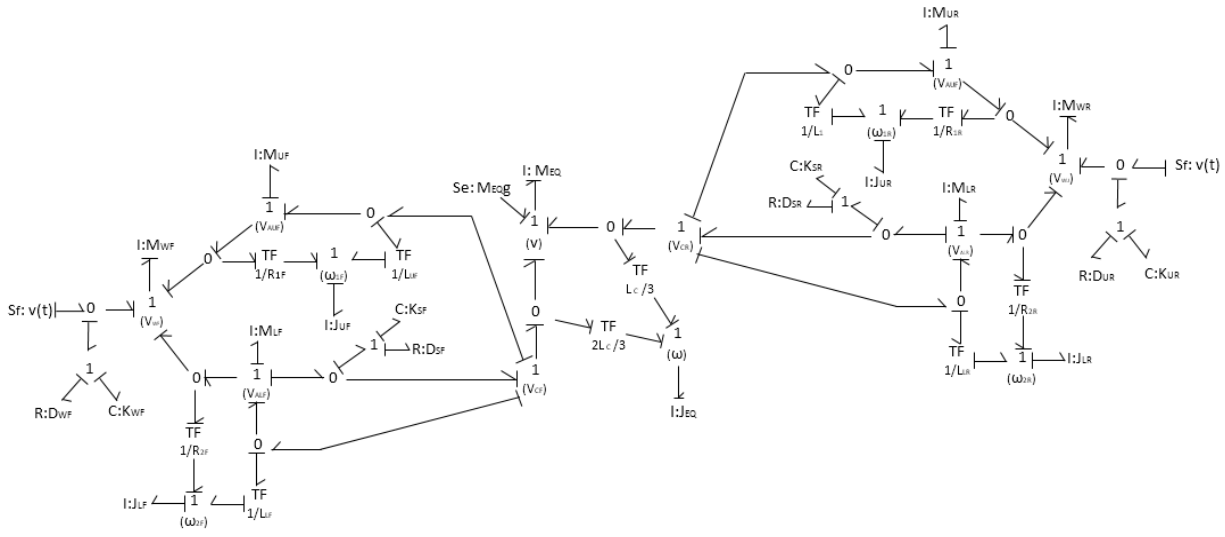

Figure 36: Causal Bond Graph

Nomenclature:

M_{eq}: Equivalent mass of vehicle
J_{eq}: Equivalent inertia of vehicle
S_e : Source of energy ($M_{eq}g$)
ω: Angular velocity at COM
V : Velocity at COM
S_f: Source of flow (road undulations)

M_{WF}: Mass of front wheel
M_{LF}: Mass of front lower A-arm
M_{UF}: Mass of front upper A-arm
J_{LF}: Inertia of front lower A-arm
J_{UF}: Inertia of front upper A-arm
V_{CF}: Velocity at front of chassis
V_{WF}:Velocity of front wheel
ω_{1F}: Angular velocity of upper front A-arm
ω_{2F}: Angular velocity of lower front A-arm
V_{AUF}: Velocity of top front A-arm
V_{ALF}: Velocity of lower front A-arm
K_{WF}: Stiffness of front wheel
K_{SF}: Stiffness of front shock
D_{WF}: Damping of front wheel
D_{SF}: Damping of front shock
$L_C/2$: Length from COM to V_{CF}
R_{1F}: Length of spindle and front lower A-arm
R_{2F}: Length of spindle and front upper A-arm
L_{UF}: Length of front upper A-arm
L_{LF}: Length of front lower A-arm

M_{WR}: Mass of rear wheel
M_{LR}: Mass of rear lower A-arm
M_{UR}: Mass of rear upper A-arm
J_{LR}: Inertia of rear lower A-arm
J_{UR}: Inertia of rear upper A-arm
V_{CR}:Velocity at rear of chassis
V_{WR}:Velocity of rear wheel
ω_{1R}: Angular velocity of upper rear A-arm
ω_{2R}: Angular velocity of lower rear A-arm
V_{AUR}: Velocity of top rear A-arm
V_{ALR}: Velocity of lower rear A-arm
K_{WR}: Stiffness of rear wheel
K_{SR}: Stiffness of rear shock
D_{WR}: Damping of rear wheel
D_{SR}: Damping of rear shock
$2L_C/3$: Length from COM to V_{CR}
R_{1R}: Length of spindle and rear lower A-arm
R_{2R}: Length of spindle and rear upper A-arm
L_{UR}: Length of rear upper A-arm
L_{LR}: Length of rear lower A-arm

Using the causal bond graph shown in Figure 36, all state variables within the system were identified as shown in Figure 37.

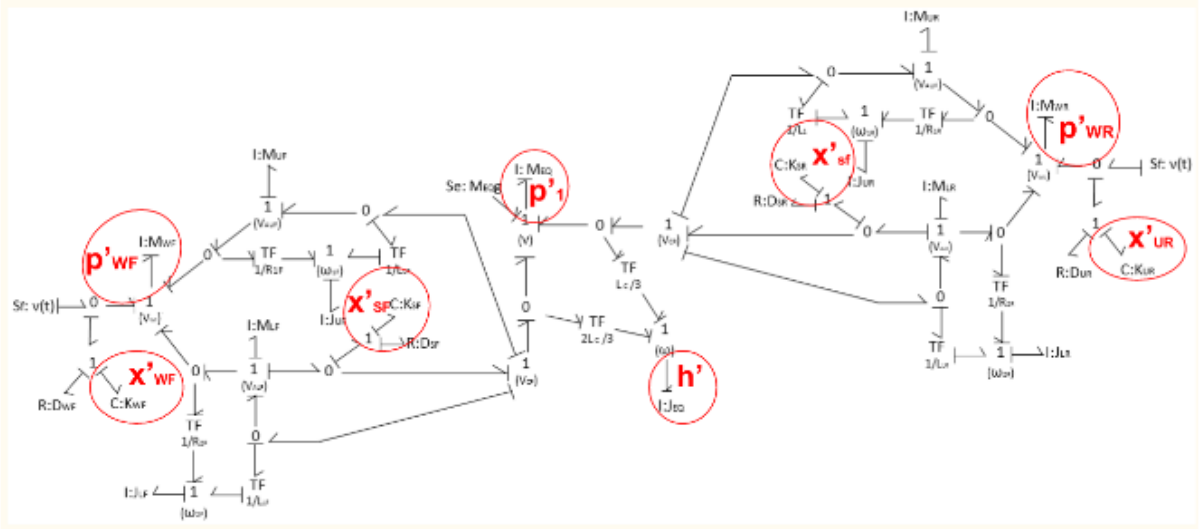

Figure 37: Causal Bond Graph with State Variables

The functions for these state variables are as follows:

States: $(x_{sf}', x_{sr}', x_{wf}', x_{wr}', p', h') = f(x_{sf}, x_{sr}, x_{wf}, x_{wr}, p, h, v_f(t), v_r(t))$

State equations were then derived and placed into Matlab. See Appendix E for the equations. Due to the complexity of the derived state equations, the Matlab code was unable to converge and; therefore, gave inconclusive results.

Frame

The frame for the Baja vehicle was designed as another MQP project by students in the 2013-2014 academic year. The design was then manufactured as part of a project at Assabet Valley Regional Technical School. Although the initial design for the frame was sound, what was manufactured deviates from the initial design which resulted in many problems that were needed to address. The largest problem that the frame caused was addressed in the aforementioned Rear Control Arms Section. In order to create a working suspension the rear of the frame had to be modified. While the frame was being modified at Hub Equipment the front tow hitch was welded to the frame in order to get the frame closer to being competition ready. The design of the tow hitch is shown in Figure 38 and the final, welded tow hitch is shown in Figure 39.

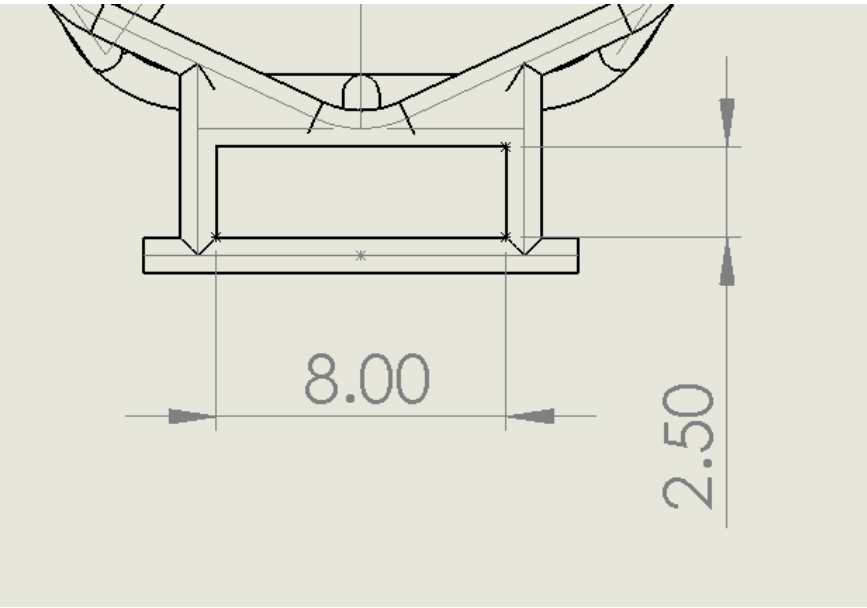

Figure 38: Drawing of Front Hitch

Figure 39: Front Hitch Point Welded by Hubb Equipment

Seating

A recycled Baja seat from the 2011 team was utilized for this year's vehicle. In order to most ergonomically mount the seat, a riser needed to be added. Using 0.25 inch 6061-T6 Aluminum, this mount was created and mounted to the chassis. 4130 Alloy Steel tabs were welded to the chassis to support the mount and a layer of rubber was added in between these components. The rubber adds damping effects and prevents galvanic corrosion that is caused when two dissimilar metals are in direct contact for extended periods of time. The seat was then mounted on top of the mount and bolted down. Based on the configuration of the cockpit within the vehicle, the seat leans against the cross support of the firewall to allow for maximum leg room. The part was then simulated under a 500lb load to calculate maximum displacement and von Mises stress.

The maximum displacement was 0.4mm and the maximum von Mises stress 23.3 MPa. Based on these numbers, the part is a successful design the meets its purpose. These results can be seen in Figure 40 and Figure 41.

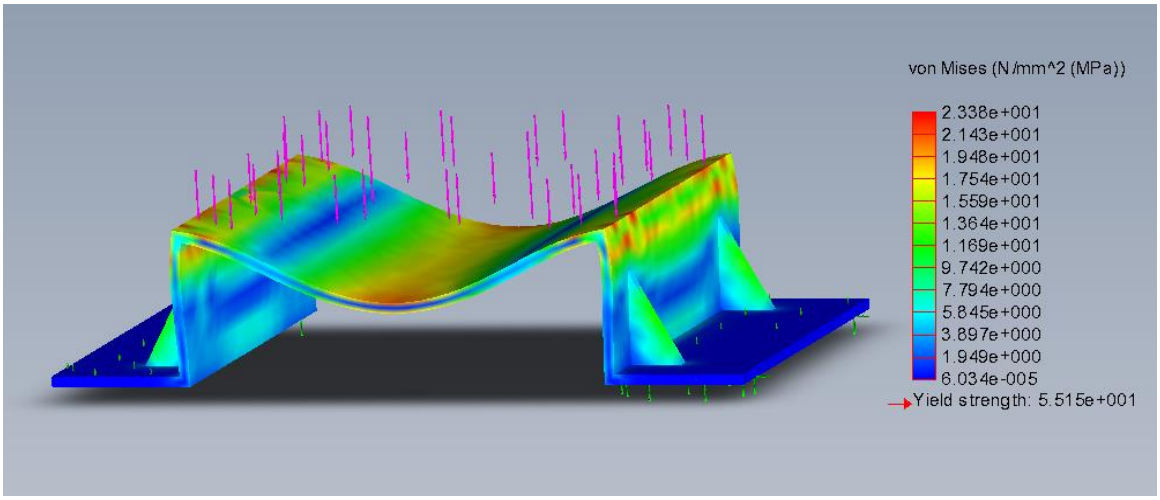

Figure 40: Maximum Displacement of Seat Mount

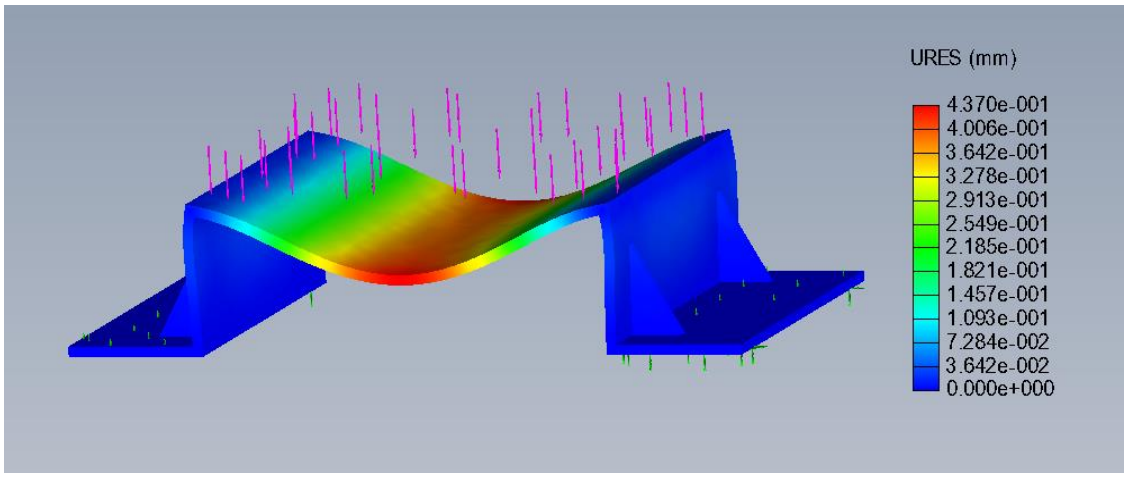

Figure 41: Von Mises Stress in Seat Mount

Body Panels

The body paneling for the vehicle was made out of a 0.0625in thick high-speed impact resistant polycarbonate sheet that was cut to fit each location. The sheets are UL972 and UL94V2 rated. The UL972 rating specifies that the sheeting can withstand a single impact at approximately 40mph and several repeated impacts at 17mph before penetration of the outer layer occurs. Given that we have calculated the maximum theoretical speed of our vehicle to be 39mph, the polycarbonate sheeting should be strong enough to protect the driver. The sheet's UL94V2 rating indicates that it has a low level flame retardance capability.

In order to manufacture the panels, a template was cut and mocked up to the location where each panel would be placed. Each template was made of cardstock due to its ability to be

easily cut while also maintaining a rigid form. Templates were then placed onto a large polycarbonate sheet, traced, and cut by hand. This provided us with flat panels which were then bent using a bending tool and adjusted until they fit properly over each location. Each panel was fastened to the frame using a combination of P-clips and screws located every 8 to 10 inches to insure body panel deflection was minimized. To finish the panel's manufacturing, they were coated with black paint on the inside surface in order to create a glossy black finish. The decision to paint the inner surface was both an aesthetic one as well as functional to prevent scratching from obstacles when the vehicle is in motion. The completed panels can be seen in Figure 42.

Figure 42: Completed Panels on Vehicle

Brakes

Based on previous work done on the vehicle by the 2014-2015 MQP team and to comply with 2016 SAE Baja Rules found in Article 11 (Appendix A), a brake pedal provided by the WPI SAE chapter was utilized. This pedal was provided with its associated master cylinders and had been mounted offset left from the center of the foot well and far enough into the frame to ensure that the master cylinders were not exposed and not susceptible to breaking in the event of a crash.

Furthermore, it was decided to continue using a floating caliper disk brake system. Due to the newly purchased spindles, new disk brakes which fit the spindles were purchased.

Drive Train

A major decision was made to incorporate a CVT into the vehicle. Previous MQP teams had stated that they found CVT's to be more detrimental than beneficial to the vehicle and have opted for alternative transmission solutions. Based on the research of Baja teams at other schools

it was agreed on that a CVT was the best option. A CVT would be mounted to the engine like in Figure 43.

Figure 43: CVT Mounted to the Model 20 Engine

Preliminary calculations demonstrated that a CVT alone would allow the vehicle to travel at a calculated speed of about 40 mph but would not produce enough torque to succeed in the hill climb event. A 12.75:1 gear ratio was needed in addition to the CVT in order to beat the hill climb challenge. The team found a salvaged high low gearbox with a 6.25:1 ratio which could be used with the CVT and an additional 2:1 ratio chain and sprocket combination to approach the required gear ratio. However, this solution was not feasible due to the designated size of the drivetrain compartment, and would fall short of the desired ratio. A second solution, which required the purchasing of a new gearbox, proved to be the most comprehensive solution. Through additional research, a Schafer H-12 Forward-Neutral-Reverse (FNR) Transaxle was found and would provide a 13.25:1 ratio. This ratio surpasses our desired 12.75:1 ratio and allowed for proper sizing within the chassis. The FNR transaxle also works as a limited slip differential which eliminated the need for an additional differential allowing for saved weight and space within the drivetrain compartment. The FNR transaxle was a high cost item that was not originally accounted for in the budget; however, after reallocating funds and working on fundraising, enough money was found to purchase the gearbox while remaining within the budget. The calculations shown below demonstrate that the Schafer FNR Gearbox would be the best option. See Figure 44 for Hill Climb calculations as well.

Theoretical Speed Calculation

$$Power\ (P) = 9.51hp = 5.231x10^3 \frac{ft \cdot lbf}{s}$$

$$Max\ Torque\ at\ 2600rpm\ (\tau_{emax}) = 13.7ft \cdot lb$$

$$Diameter\ of\ Tire\ (d_t) = 23in$$

$$Circumference\ of\ Tire\ (c_t) = \pi \cdot d_t = 6.021ft$$

$$Velocity\ of\ Engine\ (v_e) = 2800rpm$$

$$Max\ Engine\ Velocity\ (v_{emax}) = 3600rpm$$

$$Ratio\ of\ FNR\ Gearbox\ (r_{ds}) = 13.25$$

$$Ratio\ of\ Rear\ Differential\ (r_d) = 1$$

$$Maximum\ CVT\ Ratio\ (r_{CVT}) = 3$$

$$Minimum\ CVT\ Ratio\ (r_{CVT2}) = 0.5$$

$$Bearing\ Efficiency\ (\eta_b) = 0.99$$

$$Gear\ Efficiency\ (\eta_g) = 0.98$$

$$CVT\ Efficiency\ (\eta_{CVT}) = 0.80$$

$$Density\ of\ Air\ (\rho_{air}) = 0.07489\frac{lb}{ft^3}$$

$$Assumed\ Coefficient\ of\ Drag\ (c_d) = 1.2$$

$$Significant\ Area\ (A_{fire}) = \frac{1ft^2}{144in^2} \cdot [22.95in \cdot 30in + 2(18in \cdot 14in + 6in \cdot 14in)] = 9.448in^2$$

$$Maximum\ Theoretical\ Speed\ (v_{max}) = \sqrt[3]{\frac{2 \cdot P \cdot \eta_g \cdot \eta_b}{\rho_{air} \cdot (A_{fire \cdot c_d})}} = 49.583mph$$

Torque and Speed Calculation for FNR Gearbox

$$Actual\ Drive\ Ratio\ (r_{actual}) = r_{ds} \cdot r_{CVT} = 39.75$$

$$Maximum\ Torque\ from\ CVT\ and\ FNR(\tau_{max}) = \tau_{emax} \cdot r_{actual} \cdot \eta_{CVT} \cdot \eta_g = 426.947lb \cdot ft$$

$$Actual\ Maximum\ Speed\ (v_{actual}) = \frac{v_{emax} \cdot c_t}{r_{actual}} = 37.2mph$$

Hill Climb Calculations

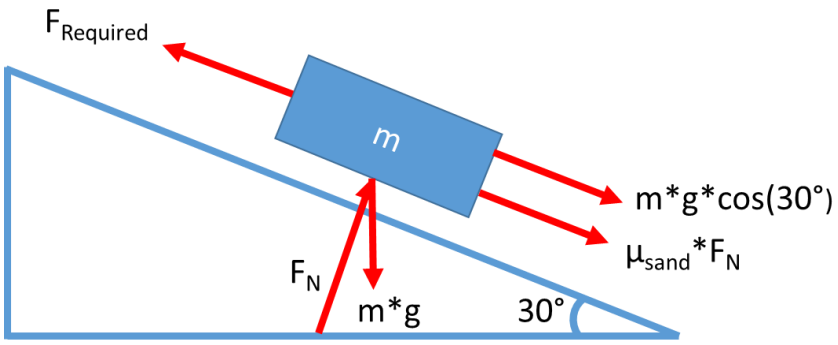

Figure 44: Visualization of Hill Climb

$$Mass\ of\ Car\ (m) = 575lb$$

$$Rolling\ Friction\ of\ Sand\ (\mu_{sand}) = 0.28$$

$$Force\ Required\ for\ Hill\ Climb\ (F_{required}) = m \cdot \sin(30) + m \cdot \cos(30) = 426.90lb$$

$$Torque\ Required\ for\ Hill\ Climb\ (\tau_{required}) = F_{required} \cdot \frac{d_t}{2} = 409.1ft \cdot lb$$

Drivetrain Modifications

The purchase of the FNR resulted in the need for some considerations to ensure proper fitment of the entire drivetrain. First, the driven clutch of the CVT needed to be bored in order to fit the input shaft of the FNR. The bore of the driven CVT clutch was 0.75 inches whereas the input shaft of the FNR was 0.875 inches. The required bore length was about 4.72 inches**,** to ensure that the entire input shaft could fit the driven clutch of the CVT. Figure 45 and Figure 46 show drawings of the original and modified CVT clutch flange respectively.

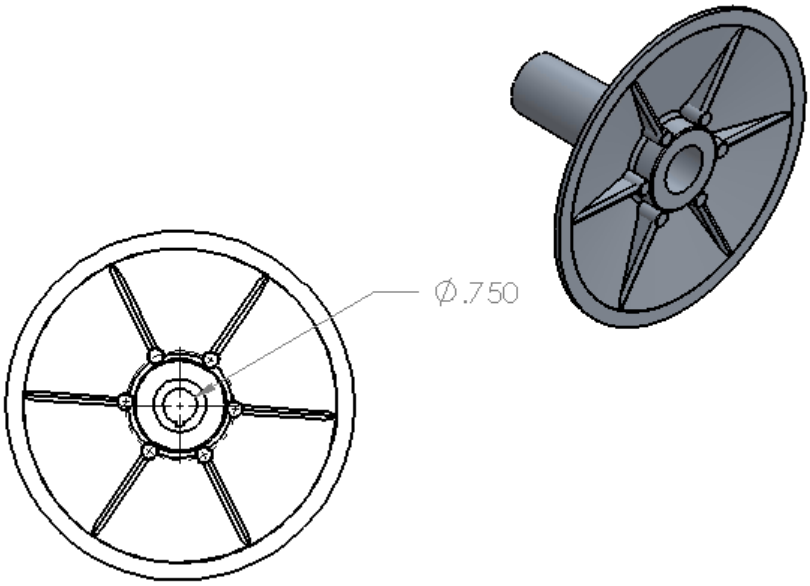

Figure 45: Drawing of Original Drive CVT Flange

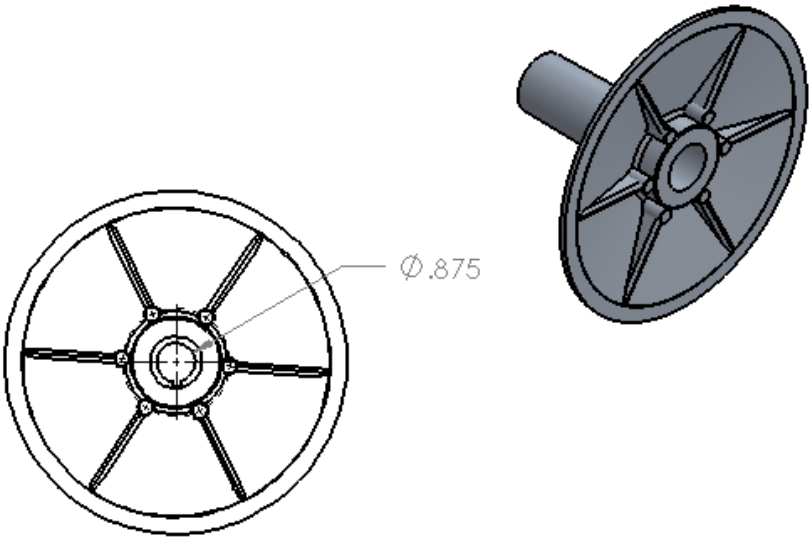

Figure 46: Drawing of Modified CVT Flange

The initial machining technique was to bore the CVT using a boring bar in a Haas ST-30SSY Y-axis CNC Lathe. However, significant deflection of the boring bar occurred resulting in variable bore dimension through the part. Next, with advice from Mikhail Tan, a lab machinist at WPI, it was decided to use a 0.875 inch drill on a manual lathe and ream the CVT to obtain a good finish at the appropriate size. Once the CVT was bored, a 0.25 inch keyway was broached in the CVT to allow the CVT to interlock with the FNR. Figure 47 shows the finished bored CVT and Figure 48 shows the fitment of the driven clutch of the CVT and the FNR input shaft.

Figure 47: Bored CVT

Figure 48: CVT Attached to FNR

The output of the FNR utilizes two splined features that could be attached to the Baja's half shafts. In order to use as many components that were already in stock and to limit the need for unnecessary redesign, the team decided to use the half shaft and spindles purchased by the previous year's MQP. The half shaft splines were incompatible with the splined FNR and an adapter needed to be made. The FNR came with the necessary female spline for its output shaft as shown in Figure 49.

Figure 49: FNR Female Spline

The female spline was welded into a 1.5 inch long steel tube which was then welded to the half shafts themselves. This solution not only allowed for the mating of the FNR to the half shaft, but also allowed the half shafts to be elongated allowing them to be properly seated inside of the spindle. Next, it was determined that the half shafts needed to be repurchased due to modifications made by previous MQPs. Again, in order to use the in stock spindles and to limit suspension redesign, the team opted to move forward with using the same half shaft type as last year. Figure 50 shows a detailed view of the half shaft with the welded adapter and Figure 51 shows how the FNR fits with the finished half shafts.

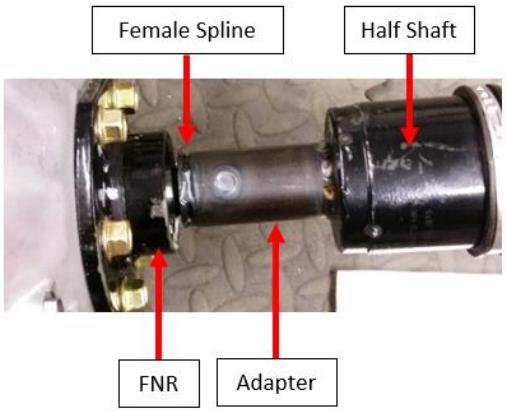

Figure 50: Detailed View of Half Shaft with Adapter

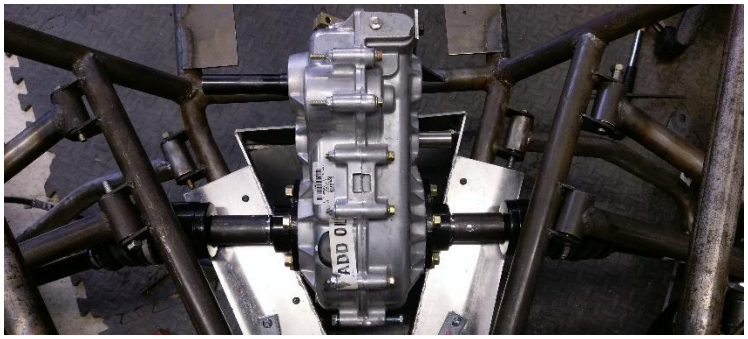

Figure 51: Fitment of Half Shafts with FNR

Drivetrain Mounting

Two major mounts were required to properly fix the engine, CVT, and FNR to the chassis. The first mount required was an engine mount that held the engine in place and the second mount was an FNR mount which would secure the FNR in place and allow for the drive clutch and driven clutch to be attached via a belt. In order to minimize overall weight of the car it was decided that the mounts would be made from 0.125 inch 6061-T6 aluminum except for recycled portions of the engine mount which would be made of 0.250 inch 6061-T6 aluminum.

The base of the engine mount was reused in order to save material as well as time. Modifications were made to allow it to fit within the chassis and to hold the engine in a different orientation than last year. Figure 52 shows the design of the engine mount.

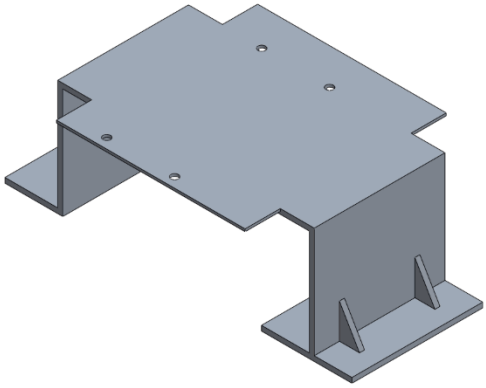

Figure 52: Engine Mount Drawing

The engine mount's structural integrity was tested through SolidWorks simulation using a 500 lb maximum load. Figure 53 and Figure 54 show the maximum displacement of 0.617mm and von Mises stresses of 2.48 MPa that were simulated.

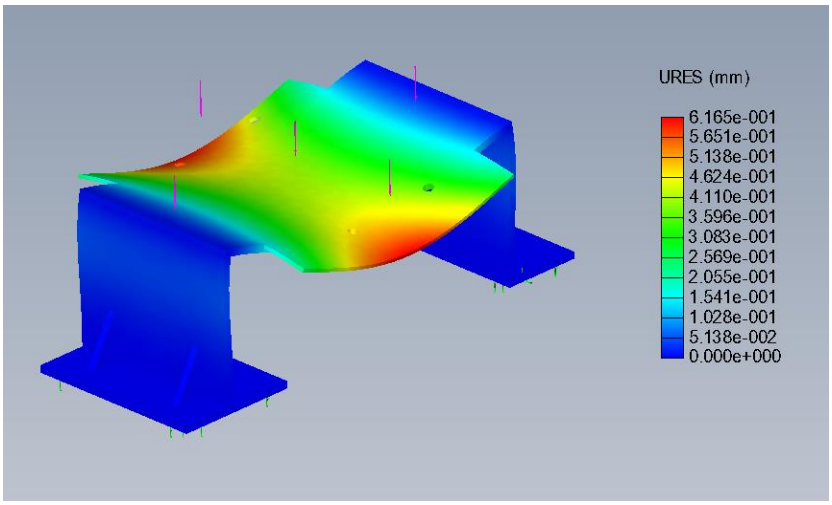

Figure 53: Maximum Displacement of Engine Mount

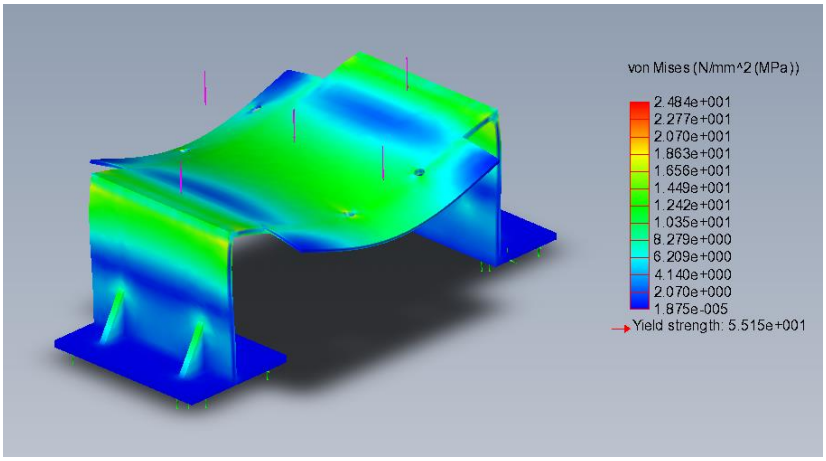

Figure 54: Von Mises Stress of Engine Mount

Since the engine mount was mostly reused from the previous MQP and in order to keep the engine's mass as close to the chassis as possible to lower the entire car's center of mass, the FNR mount was designed to recess about 3.5 inches below the chassis. The mount was designed to follow the same path as the chassis in order to allow for easy mounting. Additionally, the mount was completely enclosed with one wall only partially sealed to keep debris and water from collecting in it. The FNR mount design is shown in Figure 55.

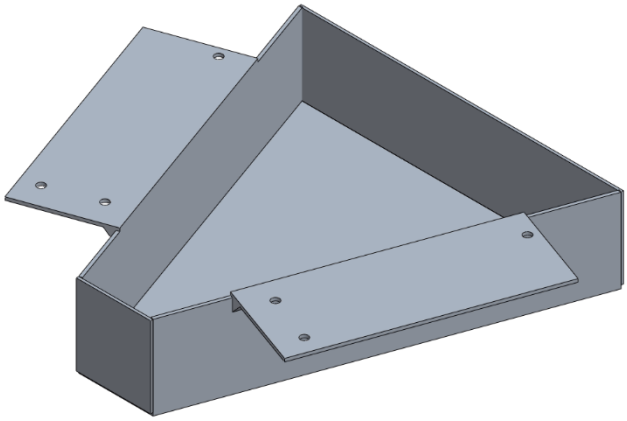

Figure 55: FNR Mount CAD Model

The FNR mount's structural integrity was tested through SolidWorks simulation using a 500 lb maximum load. Figure 56 and Figure 57 show the maximum displacement of 0.12 mm and von Mises stresses of 4.10 MPa that were simulated.

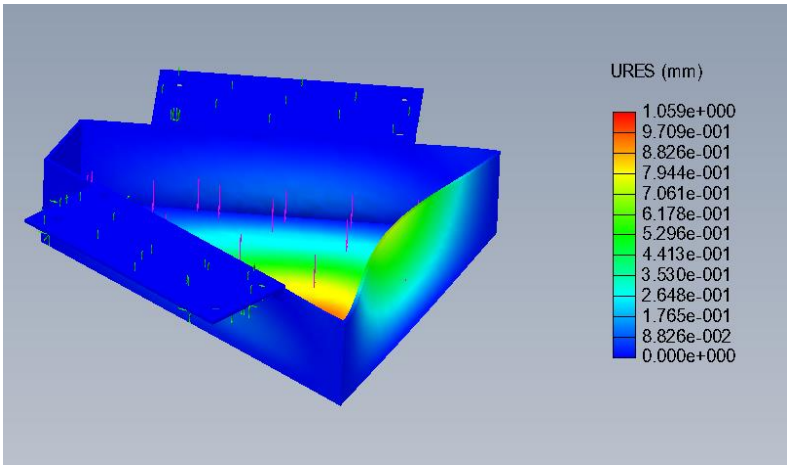

Figure 56: Maximum Displacement of FNR Mount

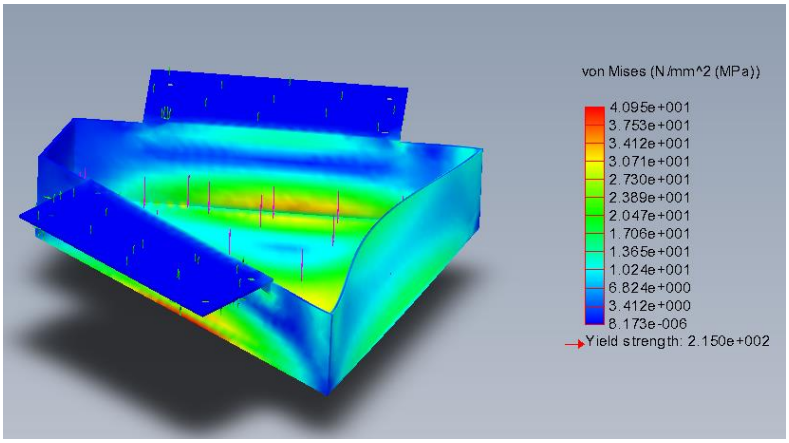

Figure 57: Von Mises Stress of FNR Mount

Next, three tabs were mounted to the FNR and chassis in order to secure the FNR in place. The first tab (front tab) was a 0.125 inch steel tab that was welded directly to the chassis and mounted to the FNR via the two FNR mounting locations provided with the FNR. The second and third (rear tabs) tabs were made from 0.125 inch angle aluminum and were mounted directly to the FNR mount via two bolts and fixed to the FNR via one of the FNR sealing bolts. This would ensure that the FNR does not move during use, Figure 58 shows the front tab and Figure 59 shows the rear tab.

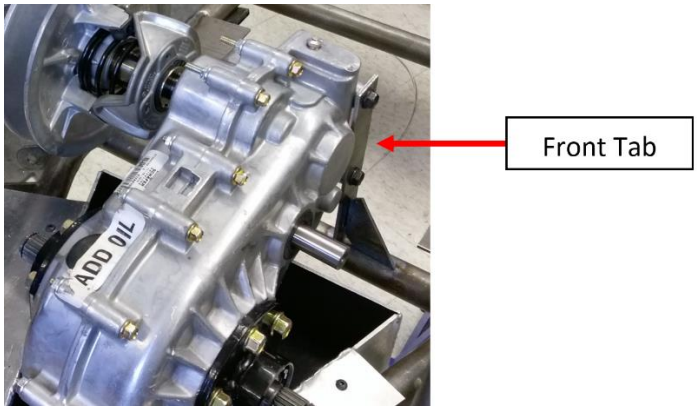

Figure 58: Front FNR Mounting Tab

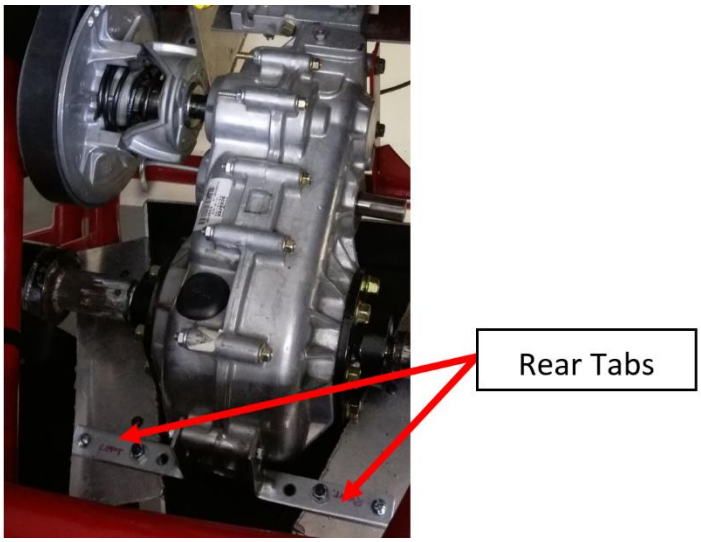

Figure 59: Rear FNR Mounting Tabs

The FNR and Engine mounts were attached to the chassis by welding steel tabs to the chassis and bolting the respective mounts to the steel tabs. 0.0325 inch thick rubber sheet was placed between the mounts and the steel tabs in order to both limit vibrations caused by vehicle operation and to reduce the chances of galvanic corrosion as similarly stated in the “Seating” section. Figure 60 shows the tabs used to mount the Engine and FNR mount to the chassis.

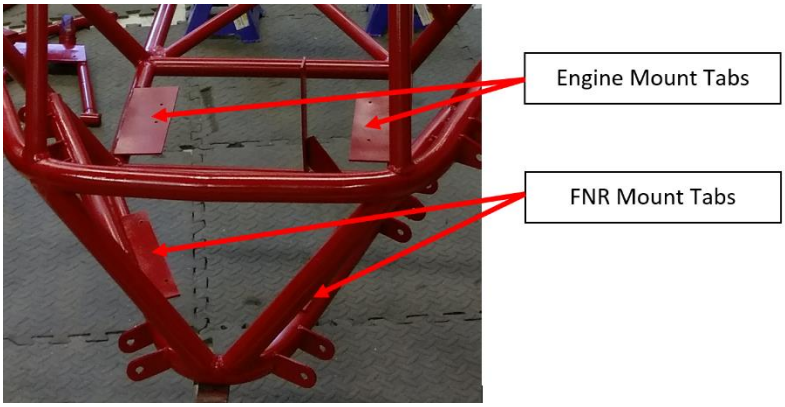

Figure 60: Engine and FNR Mount Mounting Tabs

Drivetrain Orientation

The drivetrain area consisted of the Engine, CVT, FNR, and half shafts. In order to fit all components in the allotted area and to allow all components to properly fit together, the engine needed to be raised about 6.5 inches and the FNR needed to be lowered 3.5 inches as discussed before. The engine was mounted at the front of the drivetrain compartment, closest to the firewall. The drive clutch of the CVT was connected directly to the output shaft of the engine and was mated with the engine with a 0.1875 inch square key. The drive clutch of the CVT was mated with the driven clutch of the CVT using a 9.13 inch (center to center) belt purchased with the CVT. Next, the driven clutch of the CVT was mounted to the driven shaft of the FNR with a 0.25 inch square key (as discussed earlier) and the FNR was mounted to the half shafts using the female spline and adapter discussed earlier. A SolidWorks assembly of the drivetrain demonstrates of the orientation of the engine, CVT, and FNR is shown in Figure 61.

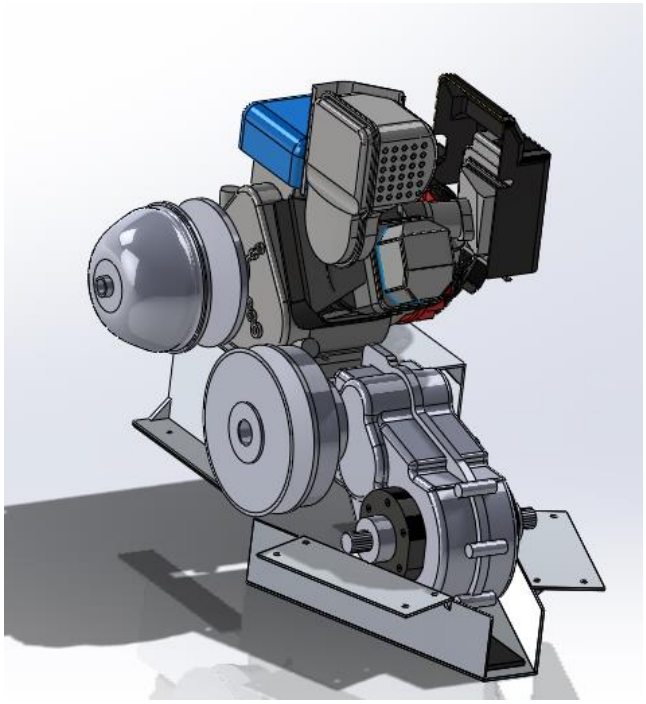

Figure 61: Drivetrain Orientation

The final, in car orientation of the drivetrain is shown in Figure 62.

Figure 62: Final Orientation of Drivetrain

Throttle Assembly

The final consideration that was made for the drivetrain was the creation of the drive train throttle assembly. This assembly consisted of the foot control, throttle cable, and throttle cable engine mount. The first modification was the addition of a torsion spring in order to force the throttle cable and gas pedal to return to their resting, home position after the foot control was released. This modification was crucial in assuring that the throttle would never become stuck in the open position. Next, the foot control linkage was modified. This modification moved second crank and coupler pinning point 0.25 inches lower than its original location. This allowed for a gain in throttle throw of about 0.5 inches. Figure 63 and Figure 64 show a PMKS simulation of the unmodified and modified foot control linkage. Although a difference of 0.5 inches in throw may not seem appreciable, it accounts for about one third of the entire available throw, making it the difference between reaching full throttle at 3800 rpm or plateauing at 2600 rpm. The modified foot control is shown in Figure 65.

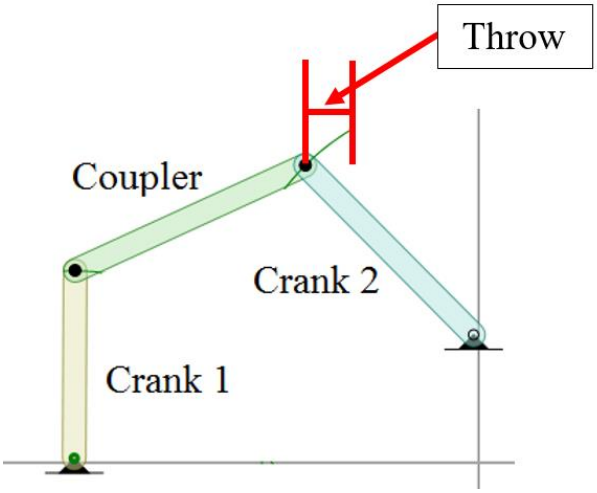

Figure 63: Unmodified Foot Control Linkage

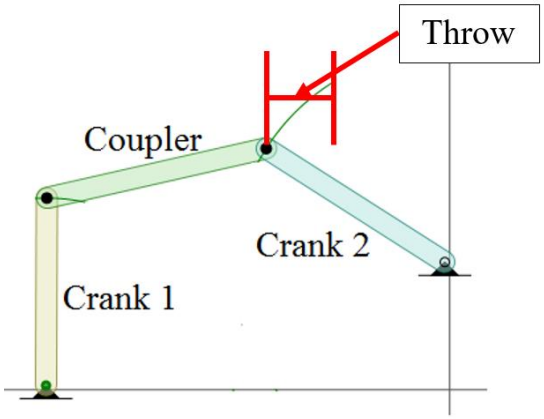

Figure 64: Modified Foot Control Linkage

Figure 65: Modified Foot Control

Next, a new throttle cable was used because the one from the previous year showed extreme wear and was not in working order. The new throttle cable utilized a mechanical stop which adjusted where the foot control's home position was. This allowed for the perfect home position orientation that allowed for maximum driver foot comfort as well as maximum throw. Finally, the throttle cable was mounted to the engine by the same mounting brackets that were used last year where jam nuts and lock washers secured the cable to the mounting bracket. Next, a 5.2 pound compression spring was inserted between the throttle cable and throttle linkage to allow for more return force adding a second degree of safety to ensure that the throttle never is stuck in the open position. The throttle cable was linked to the throttle via a bolt with a small bore which the throttle cable was threaded through. The cable was locked in place by a custom made locking piece which utilized a stopper and was secured by set screws. The throttle cable mounting system is shown in Figure 66.

Figure 66: Throttle Cable Mounting System

Circuitry

Based on the 2016 SAE Baja Rules in Article 3 which govern electrical systems, a provided series of circuit diagrams were used to determine the overall current drawn from the battery as well as how many hours the battery can operate for. The Article 3 rules can be seen in Appendix A.

Item:	Specifications:
Battery	12V; 12Ah
Reverse Light	12.8V capacity; 0.26A
Reverse Alarm	12V capacity; 0.5A
Brake Light	12V capacity; 2.9W

Table 1: Redesigned Rear, Upper Control Arms

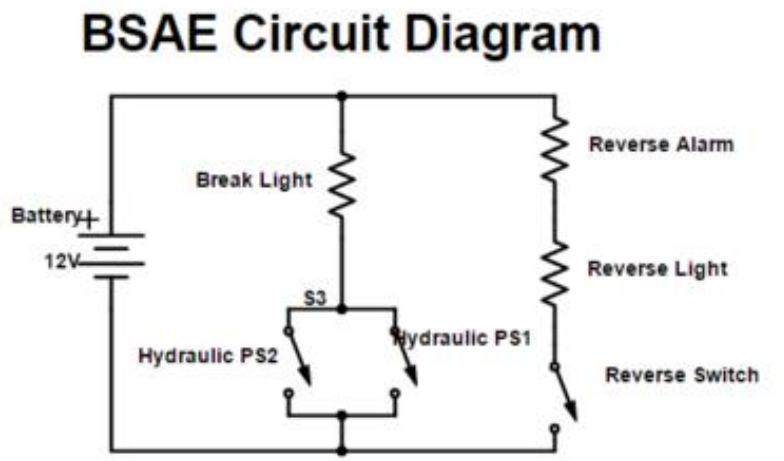

Figure 67: BSAE Circuit Diagram

By using the idea that current cannot be stored in a series circuit, it was deduced that approximately 0.5A was required to power the series connection of the reverse light and alarm. The current drawn from the brake light also needed to be determined. This was calculated via Figure 67 and the following equations:

$$Voltage = V$$

$$Current = I$$

$$Power = I * V$$

$$12W = I * 12V$$

$$I = 0.2417A$$

In order to determine the overall current of both sections, the calculated current was added to the known current of the reverse alarm and light.

$$I_{eq} = I_{brake} + I_{reverse}$$

$$I_{eq} = 0.24A + 0.5A$$

$$I_{eq} = 0.74A$$

Given that the battery is rated to last for 12Ah, we divided this number by the equivalent current value to find that with a full charge, the battery will last for approximately 16.179 hours. Since the brake light, reverse light, and reverse alarm will not be continuously used, the battery should last well beyond the calculated time. It is important to note that this battery should be sufficient at powering all current on-board systems and has the potential to power additional systems if desired.

Another requirement as of the 2016 SAE Baja Rules regarding electrical systems is that the vehicle must be equipped with two kill switches. These switches must be in series and are depicted in Figure 68. The kill switch circuit must remain independent of the brake light, reverse light, and reverse alarm.

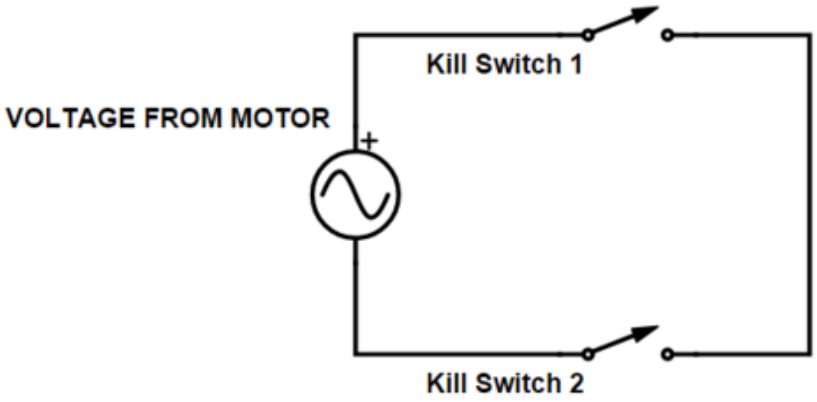

Figure

Figure 68: Kill Switch Circuit Diagram

Recommendations and Conclusions

Based on our results, there are numerous things areas for the continuation of this project next year. This year the main focus was to complete a running vehicle.

Suspension

The lower rear control arms were salvaged from the 2014-2015 MQP Baja team for monetary reasons and time constraints. It is our recommendation that a new design be created so that they better fit the needs of the competition. Currently, the control arms are large and in the way of the entire rear section of the vehicle.

The front suspension also needs an update. We were able to modify and salvage control arms from the previous year but there are a few upgrades that the system absolutely needs. Currently the camber is optimal in the system, but the caster is a little off due to the lack of space between the shock and the upper A-arm. To fix this, the mounting tabs for the shock on both the chassis and A-arm need to be translated 3 to 4 inches toward the rear of the vehicle. Once the shocks are translated, the upper A-arm also needs to be translated toward the rear 2 to 3 inches. An overall redesign of the A-arms may also be a beneficial solution in order to relocate the ball joints in the center of their respective A-arms to prevent the conflict between the brake calipers and the A-arms when the wheel is fully turned.

Shifting Linkage

Currently, the second stage of the drivetrain has the capability to operate in forward, neutral, and reverse gears. Currently, they can only be switched when the vehicle isn't running because the mechanism cannot be accessed safely otherwise. Part of the reason why the FNR gearbox was acquired was because of its reverse gear capabilities and a linkage to access this capability while the car is running with one operator on the competition course would be ideal.

Additional Safety Features

There are a number of small features that need to be added to the vehicle that are required for competition. A brake light, reverse light, reverse alarm, and fire extinguishers with mounts need to be added per SAE Baja specification. Based on the ever changing specifications, the correct parts and locations for mounting can be found in the competition specifications list online. Furthermore, for making a more comfortable and safe vehicle seat belt mounting tabs and a head rest are recommended.

Body Panels

The body panels are currently mounted onto the vehicle via p-clips. The issue with p-clips is that they allow for slight rotation along the tubing that the panel is secured to. While having multiple points to secure the panels helps to reduce this rotation, it still allows for several degrees of movement. To fix this, we recommend welding tabs onto the frame at each mounting location. This will eliminate any movement in the panels as well as make the car look more aesthetically pleasing.

Rear Tow Hitch

An additional feature required so that the vehicle meets competition specifications is a rear tow hitch. A list of requirements for the rear hitch can be found in Section B4.2.2 in Appendix A.

Steering Wheel Adapter

The steering wheel in the vehicle features several points at which there are fittings and set screws holding the column together. At the end of the steering column, prior to intersecting the steering wheel, the column attaches into an adapter that then mounts onto the steering wheel. Due to manufacturing tolerances, this adapter is slightly loose when mounted onto the steering column and allows for movement. We recommend manufacturing a new adapter for the steering wheel with tighter tolerances to alleviate this problem.

Brakes

For monetary reasons, we opted to utilize the brakes purchased by last year's MQP team. The brake dual master cylinder orientation is not ideal for mounting in our vehicle due to space restrictions. In order to fit the brake pedal far enough forward to ensure a comfortable placement for the driver, a new brake pedal that has its master cylinders mounted above the pivot point should be purchased and mounted.

Appendix A: Relevant 2016 SAE Baja Competition Rules

Article 3: Electrical System

Section B3.1 General Electrical System Overview NEW
The electrical system must include at least two kill switches, a brake light, and a battery power source. The kill switches must deactivate the engine ignition. The brake light, any reverse light and alarm, must operate regardless of the kill switch setting. The brake light, any reverse light and alarm, must be powered and functional at all times. Cut-out or disabling switches to the brake light and reverse light (if so equipped) are prohibited.

Section B3.3.1 Kill Switch – Type NEW
The kill switches must be one of the following:

(A) 01-171 Ski-Doo kill switch

(B) Aftermarket WPS#27-0152 or 27-0124

(C) A Stock Polaris # 4110106

Section B3.6 Reverse Light and Alarm NEW
Vehicles with reverse must be equipped with a backup light marked with an SAE "R" on the lens and be of LED design, equal to, or exceed the SAE standard J759. The reverse light must be mounted at a minimum of 70 cm (27.6 in) above the ground. Vehicles with reverse must also be equipped with a backup alarm. The alarm must be rated per SAE standard J1741 or J994 and sound whenever the vehicle is in reverse.

Article 4: Towing Hitch Point

Section B4.2.2.
Towing plate Minimum / Maximum thickness - 3.18mm (.125in) / 9.5mm (.375in)
Hole diameter Minimum / Maximum - 25.4mm (1.0in) / 31.75mm (1.25in)
Radial clearance Minimum / Maximum from hole - 15.875mm (.625in) / 25.4mm (1.0in)
Hole to tube Minimum / Maximum clearance - 19.0mm (.75in) / 25.4mm (1.0in)
Hitch plate Minimum width where connected to frame - 76.2mm (3.0in)

See Figure 69 for more detail.

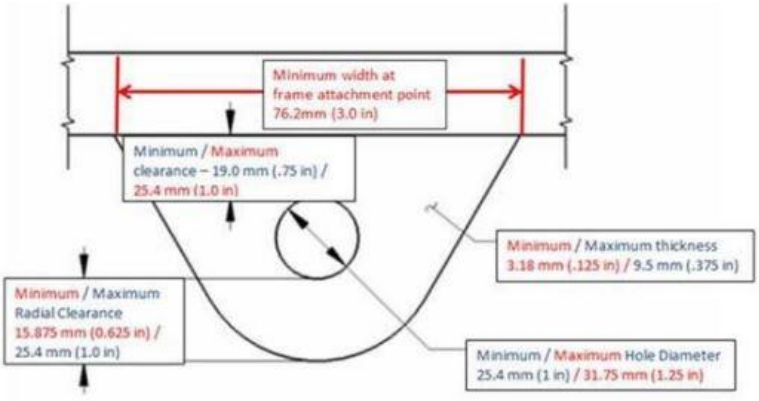

Figure 69: Rear Tow Hitch Point Drawing

Article 11: Braking System

Section B11.1 Foot Brake

The vehicle must have hydraulic braking system that acts on all wheels and is operated by a single foot pedal. The pedal must directly actuate the master cylinder through a rigid link (i.e., cables are not allowed). The brake system must be capable of locking ALL FOUR wheels, both in a static condition as well as from speed on pavement AND on unpaved surfaces.

Section B11.2 Independent Brake Circuits

The braking system must be segregated into at least two (2) independent hydraulic circuits such that in case of a leak or failure at any point in the system, effective braking power shall be maintained on at least two wheels. Each hydraulic circuit must have its own fluid reserve either through separate reservoirs or by the use of a dammed, OEM-style reservoir.

Appendix B: Shock and Spring Prices

Table 1: Polaris Shocks and Springs

Description:	University Price (Individual):	Retail Price (Individual):
Front Suspension:		
7043761 Shock – SACHS 16.3" (Ext) x 5.3" (Stroke) - 2.0" Body	$68.00	$112.99
7043809-458 Spring 115#/IN, 11.75" Length, 2.06" ID, Black	$21.00	$51.99
525376 Cam, Adjusting Spring	$2.00	$4.66
5251753 Retainer Spring	$3.00	$5.99
Rear Suspension:		
7043759 Shock – SACHS 19.0" (Ext) x 6.7" (Stroke) - 2.0" Body	$50.00	$81.99
7043760-458 Spring, 185#/IN, 12.25" Length, 2.06" ID, Red	$32.00	$78.99
5253768 Cam, Adjusting, Spring	$2.00	$4.66
5251753 Retainer, Spring	$3.00	$5.99
Total:	$362.00	$694.52

Table 2: Fox Shocks and Springs

Description:	Price (Set):
FLOAT 13.0” X 2.8”	$521.25
FLOAT 16.2” X 4.5”	$521.25
FLOAT 19.8” X 6.2”	$521.25

Table 3: Comparative Analysis of Fox, Polaris, and Rad-Flo Shocks and Springs

Manufacturer	Type	Diameter (in)	Maximum Load (lbs)	Total Cost
Fox	Air	1.659	498	$1042.50
Rad-Flo	Air	2.0	900	$940.00
Rad-Flo	Coil	2.0	400 (w/o Spring)	$1020.00
Walker Evans	Coil	2.0	500 (w/o Spring)	$740.00
Polaris	Coil	2.06	300 (w/o Spring)	$362.00

Appendix C: Vehicle Speed and Torque with Final Drive Table

RPM	CVT Ratio	Final Reduction	Engine Torque (ft. lb)	Car Speed (mph)	Torque (ft. lb.)
100	3	39.75		0.057559245	0
200	3	39.75		0.115118491	0
300	3	39.75		0.172677736	0
400	3	39.75		0.230236981	0
500	3	39.75		0.287796226	0
600	3	39.75		0.345355472	0
700	3	39.75		0.402914717	0
800	3	39.75		0.460473962	0
900	3	39.75		0.518033208	0
1000	3	39.75		0.575592453	0
1100	3	39.75		0.633151698	0
1200	3	39.75		0.690710943	0
1300	3	39.75		0.748270189	0
1400	3	39.75		0.805829434	0
1500	3	39.75		0.863388679	0
1600	3	39.75		0.920947925	0
1700	3	39.75		0.97850717	0
1800	3	39.75	13.2	1.036066415	1133.352
1900	3	39.75	13.2	1.09362566	1133.352
2000	3	39.75	13.7	1.151184906	1176.282
2100	3	39.75	13.7	1.208744151	1176.282
2200	3	39.75	14.1	1.266303396	1210.626
2300	3	39.75	14.1	1.323862642	1210.626
2400	3	39.75	14.3	1.381421887	1227.798
2500	3	39.75	14.3	1.438981132	1227.798
2600	3	39.75	14.45	1.496540377	1240.677
2700	3	39.75	14.45	1.554099623	1240.677
2800	3	39.75	14.45	1.611658868	1240.677
2800	2.9	38.425	14.45	1.724724115	1159.34373
2800	2.8	37.1	14.45	1.850118598	1080.76752
2800	2.7	35.775	14.45	1.989702306	1004.94837
2800	2.6	34.45	14.45	2.145699676	931.88628
2800	2.5	33.125	14.45	2.32078877	861.58125
2800	2.4	31.8	14.45	2.518216981	794.03328
2800	2.3	30.475	14.45	2.741952705	729.24237
2800	2.2	29.15	14.45	2.996886325	667.20852
2800	2.1	27.825	14.45	3.28909973	607.93173
2800	2	26.5	14.45	3.626232453	551.412

2800	1.9	25.175	14.45	4.017986097	497.64933
2800	1.8	23.85	14.45	4.476830189	446.64372
2800	1.7	22.525	14.45	5.019006855	398.39517
2800	1.6	21.2	14.45	5.665988208	352.90368
2800	1.5	19.875	14.45	6.446635472	310.16925
2800	1.4	18.55	14.45	7.400474394	270.19188
2800	1.3	17.225	14.45	8.582798705	232.97157
2800	1.2	15.9	14.45	10.07286792	198.50832
2800	1.1	14.575	14.45	11.9875453	166.80213
2800	1	13.25	14.45	14.50492981	137.853
2800	0.9	11.925	14.45	17.90732075	111.66093
2800	0.8	10.6	14.45	22.66395283	88.22592
2800	0.7	9.275	14.45	29.60189757	67.54797
2800	0.6	7.95	14.45	40.2914717	49.62708
2800	0.5	6.625	14.52	58.01971925	34.6302
2900	0.5	6.625	14.52	60.09185208	34.6302
3000	0.5	6.625	14.5	62.16398491	34.5825
3100	0.5	6.625	14.5	64.23611774	34.5825
3200	0.5	6.625	14.4	66.30825057	34.344
3300	0.5	6.625	14.4	68.3803834	34.344
3400	0.5	6.625	14.2	70.45251623	33.867
3500	0.5	6.625	14.2	72.52464906	33.867
3600	0.5	6.625	13.8	74.59678189	32.913
3700	0.5	6.625	13.8	76.66891472	32.913
3800	0.5	6.625	13.8	78.74104755	32.913

Appendix D: Hill Climb Results

Competition	Completed	Partial Completed	Total Completed	Percent Completed (%)	Percent Completed & Partially Completed (%)
Auburn 2015	73	4	99	73.74	77.80
Maryland 2015	72	5	98	73.47	78.60
Oregon 2015	43	34	100	43.00	77.00
UTEP 2015	3	66	109	2.75	63.30
Illinois 2014	15	67	119	12.61	68.90
Washington 2013	57	4	87	65.52	70.10
Rochester 2013	38	38	100	38.00	76.00

Percent Teams Completed: 44.15%
Percent Completed & Partially Completed: 73.1%
Percent Not Completed: 55.85%
Percent Not Completed & Partially Completed: 26.9%

Appendix E: State Equations from Mechatronic Analysis of Front and Rear Suspensions

$$p_{eq}' = M_{eq}*g + K_{sf}*x_{sf} + D_{sf} * \{ [(v_{wf} + (R_{2f}/L_{Lf}) * [(p_{eq}'/M_{eq}) + (2/3) * (L_c*h'/J_c)]) / (1 + (R_{2f}/L_{Lf}))] - [(p_{eq}'/M_{eq}) + (2/3) * (L_c*h'/J_c)] \} - [(1/L_{uf}) * (R_{1f}* M_{uf} * [(v_{wf} + (R_{1f}/L_{uf}) * ((p_{eq}'/M_{eq}) + (2/3) * (L_c*h'/J_c)) / (1 + (R_{1f}/L_{uf}))] - (J_{uf}/L_{uf}) * [(p_{eq}'/M_{eq}) + (2/3) * (L_c*h'/J_c)) - (v_{wf} + (R_{1f}/L_{uf}) * ((p_{eq}'/M_{eq}) + (2/3) * (L_c*h'/J_c)) / (1 + (R_{1f}/L_{uf}))])] / (1 - (R_{1f}/L_{uf})) - [(1/L_{Lf}) * (-R_{2f}* (K_{sf}*x_{sf} + D_{sf} * \{ [(v_{wf} + (R_{2f}/L_{Lf}) * [(p_{eq}'/M_{eq}) + (2/3) * (L_c*h'/J_c)]) / (1 + (R_{2f}/L_{Lf}))] - [(p_{eq}'/M_{eq}) + (2/3) * (L_c*h'/J_c)] \}) - R_{2f}* M_{Lf} * [(v_{wf} + (R_{2f}/L_{Lf}) * ((p_{eq}'/M_{eq}) + (2/3) * (L_c*h'/J_c)) / (1 + (R_{2f}/L_{Lf}))] - (J_{Lf}/L_{Lf}) * [(p_{eq}'/M_{eq}) + (2/3) * (L_c*h'/J_c)) - (v_{wf} + (R_{2f}/L_{Lf}) * ((p_{eq}'/M_{eq}) + (2/3) * (L_c*h'/J_c)) / (1 + (R_{2f}/L_{Lf}))])] / (1 - (R_{2f}/L_{Lf})) + K_{sr}*x_{sr} + D_{sr} * \{ [(v_{wr} + (R_{2r}/L_{Lr}) * [(p_{eq}'/M_{eq}) + (1/3) * (L_c*h'/J_c)]) / (1 + (R_{2r}/L_{Lr}))] - [p_{eq}'/M_{eq}) + (1/3) * (L_c*h'/J_c)] \} - [(1/L_{ur}) * (R_{1r}* M_{ur} * [(v_{wr} + (R_{1r}/L_{ur}) * ((p_{eq}'/M_{eq}) + (1/3) * (L_c*h'/J_c)) / (1 + (R_{1r}/L_{ur}))] - (J_{ur}/L_{ur}) * [(p_{eq}'/M_{eq}) + (1/3) * (L_c*h'/J_c)) - (v_{wr} + (R_{1r}/L_{ur}) * ((p_{eq}'/M_{eq}) + (1/3) * (L_c*h'/J_c)) / (1 + (R_{1fr}/L_{ur}))])] / (1 - (R_{1r}/L_{ur})) - [(1/L_{Lr}) * (-R_{2r}* (K_{sr}*x_{sr} + D_{sr} * \{ [(v_{wr} + (R_{2r}/L_{Lr}) * [(p_{eq}'/M_{eq}) + (1/3) * (L_c*h'/J_c)]) / (1 + (R_{2r}/L_{Lr}))] - [p_{eq}'/M_{eq}) + (1/3) * (L_c*h'/J_c)] \}) - R_{2r}* M_{Lr} * [(v_{wr} + (R_{2r}/L_{Lr}) * ((p_{eq}'/M_{eq}) + (1/3) * (L_c*h'/J_c)) / (1 + (R_{2r}/L_{Lr}))] - (J_{Lr}/L_{Lr}) * [(p'/M_{eq}) + (1/3) * (L_c*h'/J_c)) - (v_{wr} + (R_{2r}/L_{Lr}) * ((p_{eq}'/M_{eq}) + (1/3) * (L_c*h'/J_c)) / (1 + (R_{2r}/L_{Lr}))])] / (1 - (R_{2r}/L_{Lr}))$$

$$h' = (2/3)*L_C * K_{sf}*x_{sf} + D_{sf} * \{ [(v_{wf} + (R_{2f}/L_{Lf}) * [(p_{eq}'/M_{eq}) + (2/3) * (L_c*h'/J_c)]) / (1 + (R_{2f}/L_{Lf}))] - [(p_{eq}'/M_{eq}) + (2/3) * (L_c*h'/J_c)] \} - [(1/L_{uf}) * (R_{1f}* M_{uf} * [(v_{wf} + (R_{1f}/L_{uf}) * ((p_{eq}'/M_{eq}) + (2/3) * (L_c*h'/J_c)) / (1 + (R_{1f}/L_{uf}))] - (J_{uf}/L_{uf}) * [(p_{eq}'/M_{eq}) + (2/3) * (L_c*h'/J_c)) - (v_{wf} + (R_{1f}/L_{uf}) * ((p_{eq}'/M_{eq}) + (2/3) * (L_c*h'/J_c)) / (1 + (R_{1f}/L_{uf}))])] / (1 - (R_{1f}/L_{uf})) - [(1/L_{Lf}) * (-R_{2f}* (K_{sf}*x_{sf} + D_{sf} * \{ [(v_{wf} + (R_{2f}/L_{Lf}) * [(p_{eq}'/M_{eq}) + (2/3) * (L_c*h'/J_c)]) / (1 + (R_{2f}/L_{Lf}))] - [(p_{eq}'/M_{eq}) + (2/3) * (L_c*h'/J_c)] \}) - R_{2f}* M_{Lf} * [(v_{wf} + (R_{2f}/L_{Lf}) * ((p_{eq}'/M_{eq}) + (2/3) * (L_c*h'/J_c)) / (1 + (R_{2f}/L_{Lf}))] - (J_{Lf}/L_{Lf}) * [(p_{eq}'/M_{eq}) + (2/3) * (L_c*h'/J_c)) - (v_{wf} + (R_{2f}/L_{Lf}) * ((p_{eq}'/M_{eq}) + (2/3) * (L_c*h'/J_c)) / (1 + (R_{2f}/L_{Lf}))])] / (1 - (R_{2f}/L_{Lf})) + (1/3)*L_C * K_{sr}*x_{sr} + D_{sr} * \{ [(v_{wr} + (R_{2r}/L_{Lr}) * [(p_{eq}'/M_{eq}) + (1/3) * (L_c*h'/J_c)]) / (1 + (R_{2r}/L_{Lr}))] - [p_{eq}'/M_{eq}) + (1/3) * (L_c*h'/J_c)] \} - [(1/L_{ur}) * (R_{1r}* M_{ur} * [(v_{wr} + (R_{1r}/L_{ur}) * ((p_{eq}'/M_{eq}) + (1/3) * (L_c*h'/J_c)) / (1 + (R_{1r}/L_{ur}))] - (J_{ur}/L_{ur}) * [(p_{eq}'/M_{eq}) + (1/3) * (L_c*h'/J_c)) - (v_{wr} + (R_{1r}/L_{ur}) * ((p_{eq}'/M_{eq}) + (1/3) * (L_c*h'/J_c)) / (1 + (R_{1fr}/L_{ur}))])] / (1 - (R_{1r}/L_{ur})) - [(1/L_{Lr}) * (-R_{2r}* (K_{sr}*x_{sr} + D_{sr} * \{ [(v_{wr} + (R_{2r}/L_{Lr}) * [(p_{eq}'/M_{eq}) + (1/3) * (L_c*h'/J_c)]) / (1 + (R_{2r}/L_{Lr}))] - [p_{eq}'/M_{eq}) + (1/3) * (L_c*h'/J_c)] \}) - R_{2r}* M_{Lr} * [(v_{wr} + (R_{2r}/L_{Lr}) * ((p_{eq}'/M_{eq}) + (1/3) * (L_c*h'/J_c)) / (1 + (R_{2r}/L_{Lr}))] - (J_{Lr}/L_{Lr}) * [(p'/M_{eq}) + (1/3) * (L_c*h'/J_c)) - (v_{wr} + (R_{2r}/L_{Lr}) * ((p_{eq}'/M_{eq}) + (1/3) * (L_c*h'/J_c)) / (1 + (R_{2r}/L_{Lr}))])] / (1 - (R_{2r}/L_{Lr}))$$

$$p_{wf}' = (D_{wf}*v_{wf}') + (K_{wf}*x_{wf}) + [(1/L_{uf}) * (R_{1f}* M_{uf} * [(v_{wf} + (R_{1f}/L_{uf}) * ((p_{eq}'/M_{eq}) + (2/3) * (L_c*h'/J_c)) / (1 + (R_{1f}/L_{uf}))] - (J_{uf}/L_{uf}) * [(p_{eq}'/M_{eq}) + (2/3) * (L_c*h'/J_c)) - (v_{wf} + (R_{1f}/L_{uf}) * ((p_{eq}'/M_{eq}) + (2/3) * (L_c*h'/J_c)) / (1 + (R_{1f}/L_{uf}))])] / (1 - (R_{1f}/L_{uf})) + M_{uf} * [(v_{wf} + (R_{1f}/L_{uf}) * ((p_{eq}'/M_{eq}) + (2/3) * (L_c*h'/J_c)) / (1 + (R_{1f}/L_{uf}))] + [(1/L_{Lf}) * (-R_{2f}* (K_{sf}*x_{sf} + D_{sf} * \{ [(v_{wf} + (R_{2f}/L_{Lf}) * [(p_{eq}'/M_{eq}) + (2/3) * (L_c*h'/J_c)]) / (1 + (R_{2f}/L_{Lf}))] - [(p_{eq}'/M_{eq}) + (2/3) * (L_c*h'/J_c)] \}) - R_{2f}* M_{Lf} * [(v_{wf} + (R_{2f}/L_{Lf}) * ((p_{eq}'/M_{eq}) + (2/3) * (L_c*h'/J_c)) / (1 + (R_{2f}/L_{Lf}))] - (J_{Lf}/L_{Lf}) * [(p_{eq}'/M_{eq}) + (2/3) * (L_c*h'/J_c)) - (v_{wf} + (R_{2f}/L_{Lf}) * ((p_{eq}'/M_{eq}) + (2/3) * (L_c*h'/J_c)) / (1 + (R_{2f}/L_{Lf}))])] / (1 - (R_{2f}/L_{Lf})) - K_{sf}*x_{sf} - D_{sf} * \{ [(v_{wf} + (R_{2f}/L_{Lf}) * [(p_{eq}'/M_{eq}) + (2/3) * (L_c*h'/J_c)]) / (1 + (R_{2f}/L_{Lf}))] - [(p_{eq}'/M_{eq}) + (2/3) * (L_c*h'/J_c)] \} - M_{Lf} * [(v_{wf} + (R_{2f}/L_{Lf}) * ((p_{eq}'/M_{eq}) + (2/3) * (L_c*h'/J_c)) / (1 + (R_{2f}/L_{Lf}))]$$

$p_{wr}' = (D_{wr} * v_{wr}') + (K_{wr} * x_{wr}) + [(1/L_{Lr}) * (-R_{2r} * (K_{sr} * x_{sr} + D_{sr} * \{ [(v_{wr} + (R_{2r}/L_{Lr}) * [(p_{eq}'/M_{eq}) + (1/3) * (L_c * h'/J_c)]) / (1 + (R_{2r}/L_{Lr}))] - [p_{eq}'/M_{eq}) + (1/3) * (L_c * h'/J_c)] \}) - R_{2r} * M_{Lr} * [(v_{wr} + (R_{2r}/L_{Lr}) * ((p_{eq}'/M_{eq}) + (1/3) * (L_c * h'/J_c)) / (1 + (R_{2r}/L_{Lr}))] - (J_{Lr}/L_{Lr}) * [(p'/M_{eq}) + (1/3) * (L_c * h'/J_c)) - (v_{wr} + (R_{2r}/L_{Lr}) * ((p_{eq}'/M_{eq}) + (1/3) * (L_c * h'/J_c)) / (1 + (R_{2r}/L_{Lr}))])] / (1 - (R_{2r}/L_{Lr})) - K_{sr} * x_{sr} - D_{sr} * \{ [(v_{wr} + (R_{2r}/L_{Lr}) * [(p_{eq}'/M_{eq}) + (1/3) * (L_c * h'/J_c)]) / (1 + (R_{2r}/L_{Lr}))] - [p_{eq}'/M_{eq}) + (1/3) * (L_c * h'/J_c)] \} - M_{Lr} * [(v_{wr} + (R_{2r}/L_{Lr}) * ((p_{eq}'/M_{eq}) + (1/3) * (L_c * h'/J_c)) / (1 + (R_{2r}/L_{Lr}))] + [(1/L_{ur}) * (R_{1r} * M_{ur} * [(v_{wr} + (R_{1r}/L_{ur}) * ((p_{eq}'/M_{eq}) + (1/3) * (L_c * h'/J_c)) / (1 + (R_{1r}/L_{ur}))] - (J_{ur}/L_{ur}) * [(p_{eq}'/M_{eq}) + (1/3) * (L_c * h'/J_c)) - (v_{wr} + (R_{1r}/L_{ur}) * ((p_{eq}'/M_{eq}) + (1/3) * (L_c * h'/J_c)) / (1 + (R_{1fr}/L_{ur}))])] / (1 - (R_{1r}/L_{ur})) + M_{ur} * [(v_{wr} + (R_{1r}/L_{ur}) * ((p_{eq}'/M_{eq}) + (1/3) * (L_c * h'/J_c)) / (1 + (R_{1r}/L_{ur}))]$

$x_{wf}' = v_f(t) - p_{wf}/M_{wf}$

$x_{wr}' = v_r(t) - p_{wr}/M_{wr}$

$x_{sf}' = [(p_{wf}/M_{wf}) + (R_{2f}/L_{Lf}) * ((p_{eq}/M_{eq}) + (2/3) * (L_c * h/J_c))] / (1 + R_{2f}/L_{Lf}) - p_{eq}/M_{eq} + (2/3) * (L_c * h/J_c)$

$x_{sr}' = [p_{wr}/M_{wr} + (R_{2r}/L_{Lr}) * ((p_{eq}/M_{eq}) + (2/3) * (L_c * h/J_c))] / (1 + R_{2r}/L_{Lr}) - p_{eq}/M_{eq} + (1/3) * (L_c * h/J_c)$

Appendix F: Works Cited

Thomsen, D. (2015, October 15). Steering Ackerman. Retrieved December 9, 2015, from https://web.archive.org/web/20130718010927/http://www.me.ua.edu/me364/PDF/Steering_Ackerman.pdf

Burger, G., & Hendrickson, S. (2001). *Hot rodder's bible*. Osceola, Wis.: MBI Pub.

Erjavec, J. (2015). *Automotive technology: A systems approach* (6th ed.). Clifton Park, NY: Delmar, Cengage Learning.

Riley, R. (2005, February 7). Automobile Ride, Handling, and Suspension Design. Retrieved December 8, 2015, from http://www.rqriley.com/suspensn.htm

Dixon, J. (2009). *Suspension Analysis and Computational Geometry*. Chichester: John Wiley & Sons.

Atamer, B., Enjamio, J., Oliveira, S., Dale, T. V., & Wong, J. (2014, May 10). 2013-2014 WPI SAE Baja Vehicle . www.WPI.edu. Retrieved December 1, 2015, from https://www.wpi.edu/Pubs/E-project/Available/E-project-043014-170937/unrestricted/Final_Baja_MQP_Report.pdf

Crevoiserat, E. , Burgess, A., Cote, M., & Martinez, J. (2015, April 27). Design and Optimization of a Baja SAE Vehicle . www.WPI.edu. Retrieved December 1, 2015, from http://www.wpi.edu/Pubs/E-project/Available/E-project-042815-121714/restricted/Design_and_Optimization_of_an_SAE_Baja_Vehicle.pdf

Limpert, R. (2011). *Brake design and safety* (3rd ed.). Warrendale, Pa.: Society of Automotive Engineers.

Vivekanandan, N., Gunaki, A., Acharya, C., Gilbert, S., & Bodake, R. (2014). DESIGN, ANALYSIS AND SIMULATION OF DOUBLE WISHBONE SUSPENSION SYSTEM. IPASJ International Journal of Mechanical Engineering , 2(6), 1-7. Retrieved December 3, 2015, from http://ipasj.org/IIJME/Volume2Issue6/IIJME-2014-06-04-033.pdf

Wan, M. (2000). Suspension Geometry (Cont'l). AutoZine Technical School. Retrieved December 14, 2015 from http://www.autozine.org/technical_school/suspension/tech_suspension21.htm

Model 20. (n.d.). Retrieved December 14, 2015, from http://www.briggsandstratton.com/engines-racing/racing-engines/collegiate-high-school/model-20

Rahman, A., Sharif, S., Mohiuddin, A., Rashid, M., & Hossain, A. (2013). Energy efficient electromagnetic actuated CVT system. *Journal of Mechanical Science and Technology, 28*(4), 1-1. Retrieved December 15, 2015, from http://link.springer.com/article/10.1007/s12206-014-0103-9#/page-2

Boyle, C., Casola, R., Tauby, J., & Taylor, J. (2013, April 22). 2012-2013 WPI SAE Baja Vehicle . www.WPI.edu. Retrieved December 15, 2015, from http://www.wpi.edu/Pubs/E-project/Available/E-project-042213-193536/unrestricted/2012-2013_WPI_SAE_Baja_Vehicle.pdf